Energy Conversion and Management 333 (2025) 119828

Contents lists available at ScienceDirect

Energy Conversion and Management

journal homepage: www.elsevier.com/locate/enconman

Research Paper

Optimizing wind power utilization through integrated thermoelectric peak shaving

Haichao Wang [a,b,*], Jianbo Han [a], Tianyu Wang [a], Zhiwen Luo [c], Risto Lahdelma [b,d], Katja Granlund [e], Esa Teppo [e]

[a] School of Infrastructure Engineering, Dalian University of Technology, Dalian 116024, China
[b] Department of Mathematics and Systems Analysis, Aalto University, School of Science, P.O. BOX 11100, Aalto, Finland
[c] Zhiwen Luo, Welsh School of Architecture, Cardiff University, Cardiff CF10 3NB, UK
[d] Department of Mechanical Engineering, Aalto University, P.O. BOX 14100, FI-00076 Aalto, Finland
[e] Planora Oy, PL 43,Voudintie 6, 90401 Oulu, Finland

ARTICLE INFO

Keywords:
Integrated thermoelectric peak shaving
Wind power accommodation
Electric boiler
Heat pump
Combined heat and power

ABSTRACT

The integration of wind power into energy systems is a critical global challenge in the context of limited peak shaving capacity of cogeneration units, observed in many regions with high wind energy potential. This study explores thermoelectric decoupling strategies to enhance wind power utilization and improve system efficiency. Four integrated thermoelectric peak shaving schemes are investigated, including electric boiler, electric heat pump, absorption heat pump, and mechanical heat pump, each integrated with thermal energy storage. A mathematical model was developed and validated using data from a combined heat and power plant in Jilin Province, China, demonstrating its scalability and applicability. The results indicate that the mechanical heat pump and electric heat pump schemes achieved the highest net incomes, with exergic efficiencies exceeding 65 %. The electric boiler scheme achieved the highest wind power utilization, reducing the wind curtailment rate to 0.1 %. All schemes contributed to significant coal savings, with the mechanical heat pump reducing standard coal consumption by 16.91 kg/MWh of electricity and 1.22 kg/GJ of heat. Furthermore, the schemes demonstrated substantial carbon emission reductions and improvements in overall energy efficiency. These findings provide more insights into enhancing the operational flexibility of combined heat and power systems and integrating renewable energy sources, offering a scalable solution for regions seeking to transition to low-carbon energy systems.

1. Introduction

Renewable energy systems are becoming a cornerstone of the global energy transition, with wind energy playing a critical role in decarbonizing energy systems. However, wind power curtailment due to insufficient flexibility in combined heat and power (CHP) systems is a persistent issue worldwide, particularly in regions with growing renewable energy penetration. For example, China's energy structure is undergoing a swift transformation towards low-carbon. The proportion of clean energy has been steadily increasing, reaching 25.9 % of total energy consumption in 2022. However, total coal consumption still accounts for 56.2 % of the total energy consumption[1]. While the proportion of coal consumption is decreasing, it remains difficult to change coal as the primary energy source in the short term. Therefore, improving the utilization of renewable energy is imperative in response to the "peak carbon dioxide emissions, carbon neutral" policy. By the end of 2022, China's cumulative installed wind power capacity had reached 365 GW, increasing by 11.2 % compared to the previous year. However, the wind power waste remains a pressing concern[1]. District heating in northern China relies primarily on CHP units and coal-fired boilers. As the district heating area continues to expand, CHP units generate a considerable electricity while meeting user heat demands, constraining wind power's utilization and leading to severe wind curtailment issues.

Enhancing the peaking capacity of CHP units through the transformation of CHP can effectively facilitate the integration and decarbonization of renewable energy [2]. To a certain extent, the problem of wind abandonment in the 'three north' area can be alleviated. Sun et al. [3] determine the optimal thermal energy storage (TES) capacity and

* Corresponding author.
E-mail address: wanghaichao2002@163.com (H. Wang).

https://doi.org/10.1016/j.enconman.2025.119828
Received 1 July 2024; Received in revised form 26 February 2025; Accepted 18 April 2025
Available online 26 April 2025

Nomenclature

Abbreviation

CHP	Combined heat and power
TES	Thermal energy storage
CSP	Concentrated solar power
EB	Electric boiler
HP	Heat pump
EHP	Electric heat pump
AHP	Absorption heat pump
MHP	Mechanical heat pump
CON	Condensing unit

Symbols

$F_{CHP}(t)F_{CHP}(t)$ The operating cost of CHP units at time *t*, ten thousand yuan

f_if_i The operating cost of the *i* characteristic point of CHP units, ten thousand yuan

$x_i(t)x_i(t)$ The value of decision variable coding operation area in the feasible area of CHP units

$P_{CHP}(t)P_{CHP}(t)$ The electrical output of CHP units at time *t*, MW

p_ip_i The electrical output of the *i* characteristic point of CHP units, MW

$Q_{CHP}(t)Q_{CHP}(t)$ The thermal output of CHP units at time *t*, MW

q_iq_i The thermal output of the *i* characteristic point of CHP units, MW

$F_{CON}(t)F_{CON}(t)$ The operating cost of CON units at time *t*, ten thousand yuan

kk The unit power generation cost of CON units, ten thousand yuan/MW

$P_{CON}(t)P_{CON}(t)$ The CON units electrical output at *t* time, MW

$F_{HB}(t)F_{HB}(t)$ The operation cost of the peaking boiler at time *t*, ten thousand yuan

$Q_{HB}(t)Q_{HB}(t)$ The thermal output of the peaking boiler at time *t*, MW

$f_{caol}f_{caol}$ The standard coal price, yuan /t

$\eta_{HB}\eta_{HB}$ The operating efficiency of the peaking boiler, %

q_0q_0 The calorific value of standard coal, 29.27 MJ/kg

F_eF_e The heating season CHP units, CON units sales income, ten thousand yuan/year

F_hF_h The heating season sales heat income, ten thousand yuan/year

F_wF_w The revenue gained from selling wind power during heating season, ten thousand yuan/year

$F_{cost}F_{cost}$ The operating cost of the heating system in the season, ten thousand yuan /year

C_eC_e The sale of electricity power prices, ten thousand yuan

C_hC_h The sale of heat power prices, ten thousand yuan

C_wC_w The sale of wind power prices, ten thousand yuan

$P_i^{CHP}(t)P_{CHP}^i(t)$ The electrical output of the *i* CHP units at time *t*. MW

$P_j^{Con}(t)P_{CON}^j(t)$ The electrical output of the *j* CON units at time *t*. MW

$Q_D(t)Q_D(t)$ The system heat load at time *t*, MW

$P_w(t)P_w(t)$ The wind power at time *t*, MW

$F_i^{CHP}(t)F_{CHP}^i(t)$ The operating cost of the *i* CHP units at *t* time, ten thousand yuan

$F_j^{CON}(t)F_{CON}^j(t)$ The operating cost of the *j* CON units, ten thousand yuan

$F^f(t)F^f(t)$ The operating cost of the auxiliary heat source equipment, ten thousand yuan

$P_{CHP,i}(t)P_{CHP}^i(t)$ The CHP units electrical output at *t* time, MW

$P_{CHP,i}(t-1)P_{CHP}^i(t-1)$ The CHP units electrical output at *t*-1 time, MW

$P_{CHP,r}P_{CHP,r}$ The climbing power of CHP units, MW/h

$P_{CHP,max}P_{CHP,max}$ The upper limit of the electric output of CHP units, MW

$P_{CHP,min}P_{CHP,min}$ The lower limit of the electric output of CHP units, MW

$Q_{CHP,max}Q_{CHP,max}$ The upper limit of thermal output of CHP units, MW

$Q_{CHP,min}Q_{CHP,min}$ The lower limit of thermal output of CHP units, MW

$P_{CON,max}P_{CON,max}$ The upper limit of the power output of CON units, MW

$P_{CON,min}P_{CON,min}$ The lower limit of the power output of CON units, MW

$P_{CON,i}(t)P_{CON}^i(t)$ The CON units electrical output at *t* time, MW

$P_{CON,i}(t-1)P_{CON}^i(t-1)$ The CON units electrical output at *t*-1 time, MW

$P_{W,pre}(t)P_{W,pre}(t)$ The forecast amount of wind power at time *t*, MW

$Q_D(t)Q_D(t)$ The system heat load at time *t*, MW

$Q_i^{CHP}(t)Q_{CHP}^i(t)$ The heat produced by the *i* thermoelectric unit at time *t*, MW

$Q_f(t)Q_f(t)$ The heat supply of auxiliary heat source equipment at time *t*, MW

$E_D(t)E_D(t)$ The electrical load on the system at time *t*, MW

$Q_{TES}(t)Q_{TES}(t)$ The heat in TES at *t* time, MWh

$Q_{TES}(t-1)Q_{TES}(t-1)$ The heat in TES at *t*-1 time, MWh

$\eta_{TES,S}\eta_{TES,S}$ The heat storage efficiency of the TES, %

$Q_{TES,S}(t)Q_{TES,S}(t)$ The heat stored at time *t*, MW

$Q_{TES,R}(t)Q_{TES,R}(t)$ The heat discharged at time *t*, MW

$Q_{S,max}Q_{S,max}$ The maximum heat storage rate of TES, MW

$Q_{R,max}Q_{R,max}$ The maximum heat storage rate of TES, MW

$P_{EB}(t)P_{EB}(t)$ The power consumption of EB at time t, MW

$P_{EB,max}P_{EB,max}$ The maximum operating power of EB, MW

$Q_{EB}(t)Q_{EB}(t)$ The thermal output of EB at time *t*, MW

$\eta_{EB}\eta_{EB}$ The operating efficiency of EB, %

$P_{EHP}(t)P_{EHP}(t)$ The EHP power consumption at *t* time, MW

$P_{EHP,max}P_{EHP,max}$ The maximum power of EHP, MW

$Q_{EHP}(t)Q_{EHP}(t)$ The EHP heating output at *t* time, MW

$Q_{q,AHP}(tQ_{q,AHP}(t)$ The AHP drive steam heat at *t* time, MW

$Q_{q,AHP,max}Q_{q,AHP,max}$ AHP's maximum drive steam heat, MW

$Q_{AHP}(t)Q_{AHP}(t)$ The heating output of AHP at *t* time, MW

$P_{MHP}(tP_{MHP}(t)$ The MHP drive power at *t* time, MW

$\eta_T\eta_T$ The transmission efficiency between the turbine and the generator, %

$\eta_M\eta_M$ The generator efficiency, %

$P_{MHP,max}P_{MHP,max}$ The maximum power of MHP, MW

$Q_{MHP}(t)Q_{MHP}(t)$ The heating output of MHP at time *t*, MW

$F_{tz}F_{tz}$ The cost of amortizing the initial investment of the auxiliary heat source equipment to the entire life cycle of the equipment, ten thousand yuan /year

C_fC_f The initial investment per unit capacity equipment, ten thousand yuan /MW

R_fR_f The new peak load equipment capacity, MW

$C_{TES}C_{TES}$ The cost per cubic meter of TES construction, ten thousand yuan $/m^3m^3$

$V_{TES}V_{TES}$ The capacity of TES,m^3m^3

nn The service life of the equipment is, years, assuming that the service life is 20 years

$\eta_W\eta_W$ The system curtailment rate, %

$P_{W,pre}P_{W,pre}$ The forecast amount of regional wind power, MW

P_WP_W The amount of wind power connected to the system, MW

$\eta_N\eta_N$ The system's wind capacity, %

$P_{W,0}P_{W,0}$ The amount of wind power connected to the traditional CHP system, MWh

$a_0a_1a_2a_0$, a_1, a_2 The fitting coefficient of coal consumption of CON units

$b_0b_2b_3b_4b_5b_0$, b_2, b_3, b_4, b_5 The fitting coefficient of coal consumption of CHP units

$C_{CHP}C_{CHP}$ The carbon transaction cost of CHP units, ten thousand yuan
$\alpha\alpha$ The carbon trading price, this paper takes 50 yuan /t CO_2CO_2
$\delta_{CHP}\delta_{CHP}$ The carbon emission coefficient of CHP units, which is 0.968 kg/kWh in this paper
$\gamma\gamma$ Carbon trading quota, this article takes 0.798 g/kWh
$P_{CHP,d}(t)P_{CHP,d}(t)$ The generation power of CHP units at time t under equivalent pure The condensation condition, the electric power of CHP units at time t under equivalent pure condensation condition, MW
C_vC_v The electric power reduced when the unit thermal output of CHP units is increased, MW
$C_{CON}C_{CON}$ The carbon trading cost of CON units, ten thousand yuan
$\delta_{CON}\delta_{CON}$ The carbon emission coefficient of CON units, which is taken in this paper 0.849 kg/kWh
$C_{Wind}C_{Wind}$ The carbon trading cost of wind power
$\eta_{ex}\eta_{ex}$ The exergic efficiency of system, %
$E_{out}E_{out}$ The system exited exergy, kW
$E_{in}E_{in}$ The system entered in the system, kW
$E_{f,CHP}E_{f,CHP}$ The standard coal chemical exergy, kW
B_fB_f The coal consumption of a CHP system, t
q_0q_0 The calorific value of standard coal, kJ/kg
E_RE_R The thermal exergy, kW
E_gE_g The exergy of supply water of heat supply network, kW
E_hE_h The exergy of return water of heat supply network, kW
D_wD_w The circulating water flow rate of the heat supply network, kg/s
T_0T_0 the ambient temperature, K
h_gh_g The enthalpy value of water supply of the heat supply network,kJ/kgkJ/kg
h_hh_h The enthalpy value of water return of the heat supply network,kJ/kgkJ/kg
s_gs_g The entropy of supply water of the heat supply network,kJ/(kg • K)kJ/(kg • K)
s_hs_h The entropy of return water of the heat supply network,kJ/(kg • K)kJ/(kg • K)
h_0h_0 The enthalpy of water at ambient temperature,kJ/kgkJ/kg
s_0s_0 The entropy of water at ambient temperature,kJ/(kg • K)kJ/(kg • K)
E_PE_P The electrical exergy, kW
P_PP_P The generating power of units, kW

heat release rate for the case system, enabling improved depth peaking capacity of the units and a coal consumption saving of 20.91 g/kWh for the system. Additionally, a feasible logic operation scheduling strategy for heat storage and heat release is proposed. Pablo[4] proposes an economic approach for estimating the heat accumulator volume through the historical heat load, specifically for the thermal power plant transformation. The findings indicate that increasing the TES can significantly reduce the operating hours of the CHP units' maximum generating capacity. Zhang et al. [5] demonstrated through the establishment of a model combining wind power generation and heat storage electric boilers (HSEB) for auxiliary heating that this approach possesses strong peak shaving capabilities, effectively reducing the impact of wind power fluctuations on the power grid. Ling et al. [6] conducted research on the control strategy of heat storage boilers using PLC, optimizing the operating mode of the thermal storage unit and achieving optimized control of multi–agent-based electric heat storage boilers. Cheng et al. [7] studied the model and control strategy of heat storage electric boilers, coupling them with CHP to decrease the output of the units and improve wind energy utilization. Chen et al. [8] analysis the heat storage system in thermoelectric peaking reveals that the capacity of TES decreases as the heat load increases. Getent et al. [9], utilizing population optimization, an optimal operation model of integrated heat and power is proposed. The model incorporates an extended energy hub method, which allows for the modular representation of regional energy system components. This approach takes into account the intermittency of renewable energy sources and the variability of electricity prices. Through simulation analysis, it is determined that the utilization rate of wind power can surpass 97 %. Xu et al. [10], proposed a scheme and operation scheduling strategy for concentrated solar power (CSP) power stations and electrode boilers to enhance the utilization of new energy. A numerical example analysis based on the IEEE30-node model demonstrated that the system can bolster renewable energy capacity in regional energy systems while reducing carbon emissions. The electric boiler (EB) and TES enable efficient thermoelectric decoupling. However, accurate EB power and TES capacity are necessary to ensure optimal system operation benefits. But the simulation of the transformation scheme in the literature is based on a 24-hour system, lacking a comprehensive analysis of the operational effects over the entire heating season and economic considerations.

In addition to EB, heat pumps (HP) are also commonly used for cogeneration peak shaving. The utilization of high-power heat pumps can enhance the peak shaving capacity of CHP units and enable the utilization of power plant waste heat. This approach is beneficial for reducing system operating costs and minimizing energy waste. Liu et al. [11], utilized 350 MW CHP units to quantitatively analyze the contribution of EB and HP in cogeneration peak shaving. The results showed that when EB and HP are involved in peak shaving, the minimum electric load reduction of CHP units is 124.2 MW and 71.6 MW, respectively. Gao et al. [12], established an optimization model for EB and HP participating in the frequency regulation of CHP units. The results indicated that the HP scheme can increase annual profit by 27.7 %, outperforming the 3.1 % increase achieved by EB. Wang et al. [13] used Ebsilon software to establish a model for 600 MW CHP units and analyzed the impact of thermoelectric decoupling technologies such as heat storage, EB, HP, and steam turbine transformation on the feasible range of CHP units. The study demonstrated that utilizing HP or a combination of HP and TES is the most energy-saving thermoelectric decoupling method. HP can be further categorized into electric heat pump (EHP), absorption heat pump (AHP), and mechanical heat pump (MHP) based on different driving energies. Wu et al. [14], developed a system model of AHP for recovering waste heat from thermal power plants and participating in thermoelectric peak shaving. The optimal capacity of the auxiliary heat source equipment was determined using the entropy method and comprehensive analysis of six evaluation indexes. Wang et al. [15], proposed a dynamic model of CHP based on the efficiency factor and analyzed the decoupling capability of combined AHP and EHP operation. The study revealed that EHP has a better effect when there is high heat demand and low power demand. Zhang et al. [16], introduced a series operation system of EHP and CHP units. The results showed that this new system effectively improves the operating efficiency, reduces coal consumption by 9.53 g/kWh, and decreases wind power curtailment by 10.75 %. Coskun et al. [17], studied the influence of control parameters of MHP on the performance of waste heat recovery. Experimental results demonstrated that applying MHP for waste heat recovery significantly enhances system performance. The utilization of heat pumps for collaborative peak shaving of heat and electricity improves the flexibility of CHP unit operations, enhances the thermal conditions of CHP and the stability of the heating network. However, due to the different driving energies and operating mechanisms of heat pumps, their effects on peak shaving may vary, necessitating further comparative analysis.

Addressing renewable energy integration requires innovative

approaches that integrate thermoelectric decoupling technologies and peak shaving mechanisms. While previous studies have explored isolated cases, there is a need for a comprehensive and scalable framework applicable to diverse geographic and operational contexts. At present, most of the research works are analyzed from a single perspective of heat or electricity, and lack the consideration of thermoelectric coordinated peaking. At the same time, there are few studies on the participation of multiple heat sources in thermoelectric peaking, and the analysis of joint operation technology of equipment is lacking. The novelty of this study mainly lies in maximizing the renewable energy integration considering optimal flexibility of CHP with a wider range of different power-to-heat schemes. This paper proposes a mathematical model to optimize wind power utilization and improve the flexibility of CHP systems through the integration of auxiliary heating sources and TES. Coordination of wind power grid integration is an important goal of future energy development when realizing collaborative peak shaving of heat and power [18]. Based on the previous research, this study focuses on the thermoelectric collaborative peaking approach by utilizing EB, EHP, AHP, and MHP coupled with TES. Mathematical models for different schemes are established using Matlab software to examine the impact of these schemes on renewable energy consumption. The optimum capacity of auxiliary heat source equipment was determined by net income, wind curtailment rate, exergy efficiency, coal consumption and carbon emission and the advantages of different peaking schemes were determined. By leveraging data from a thermal power plant in Jilin Province, China, this study extends its findings to inform international energy policy and operational strategies.

2. Methods

This study proposes four integrated thermoelectric peak shaving regulation schemes, including electric boiler (EB), electric heat pump (EHP), absorption heat pump (AHP), and mechanical heat pump (MHP). This section analyzes the system structure and operating mechanism of all schemes coupled with TES to explore the different renewable energy integration and peak shaving capabilities.

2.1. Analysis of integrated thermoelectric peak shaving schemes

The system configuration and operating mechanism of each peak shaving scheme will be analyzed to highlight unique features of each scheme.

2.1.1. Electric boiler coupled heat accumulator scheme

EB offer several advantages such as high operation efficiency, easy operation. Directly consuming wind power heating through EB is an important method for achieving thermoelectric decoupling and the utilization of wind curtailment [16]. Fig. 1 shows the system connection of EB coupled with TES for thermoelectric peaking. The EB directly consumes wind power to heat the return water of the primary network. This approach reduces the thermal output of CHP units while enhancing their flexible peaking capacity, meeting the heat load requirements of users. Moreover, during periods of high wind power generation at night, the extra heat produced by EB can be stored in TES. This stored heat can then be released during peak electricity demand periods during the day, alleviating the power generation strain on CHP units.

The peaking scheme of EB coupled with TES provides several advantages, such as a simple structure, minimal impact from heat load fluctuations, a wide adjustment range, and rapid response speed. The scheme can directly consume wind power heating, reduce the lower limit of power output of the unit, and provide a certain space for wind power utilization. By storing extra heat generated by EB during periods of high wind power generation, the scheme enables the efficient use of renewable energy and ensures the stability of heating.

2.1.2. Electric heat pump coupled heat accumulator scheme

The implementation of EHP for consuming surplus wind power in heating, along with replacing CHP units to undertake a portion of heat load, enhances the flexibility of CHP units for both heating and power generation. This helps improve power grid stability and creates room for wind power generation. The TES system, with its low cost and ability to store excess heat, can effectively compensate for peak heat loads and expand the output power range of CHP units [19]. Fig. 2 illustrates the system connection of EHP coupled with TES for thermoelectric peaking.

The evaporation side of EHP is relates to the condensate water circulation system to recover the low-temperature waste heat in the frozen water of the cogeneration unit to heat the return water of the primary network, reduce the thermal output of the cogeneration unit. Additionally, the EHP operates with high efficiency, effectively improving the overall energy utilization efficiency of the system.

2.1.3. Scheme of absorption heat pump coupled heat accumulator

The use of AHP for collaborative peak shaving of heat and power involves consuming a portion of the heating steam to drive the system. By absorbing low-temperature waste heat in the condensate water of the power plant for heating purposes, the energy efficiency of the system is improved. This approach effectively reduces operating costs, reduces carbon emissions, and resolves the problem of insufficient peak shaving capacity in large CHP units [20]. Fig. 3 shows the system connection mode of the AHP coupled with TES scheme. In this configuration, the

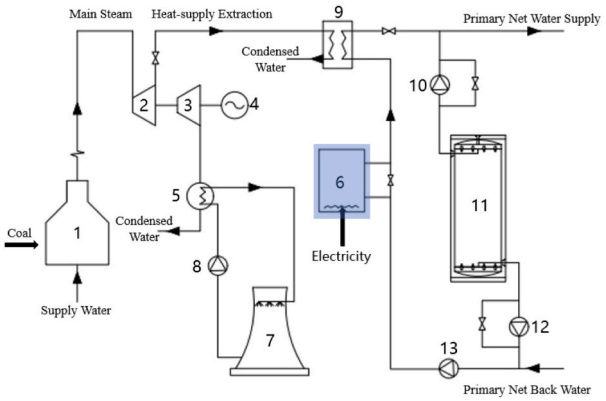

1- Coal-fired Boiler 2, 3- Steam Turbine 4- Dynamo 5- Condenser 6- Electric Boiler 7- Cooling Tower 8- Condensate Pump 9- Heat Exchanger 10, 12- Circulating Pump 11- Heat Accumulator

Fig. 1. EB coupled TES scheme system structure diagram.

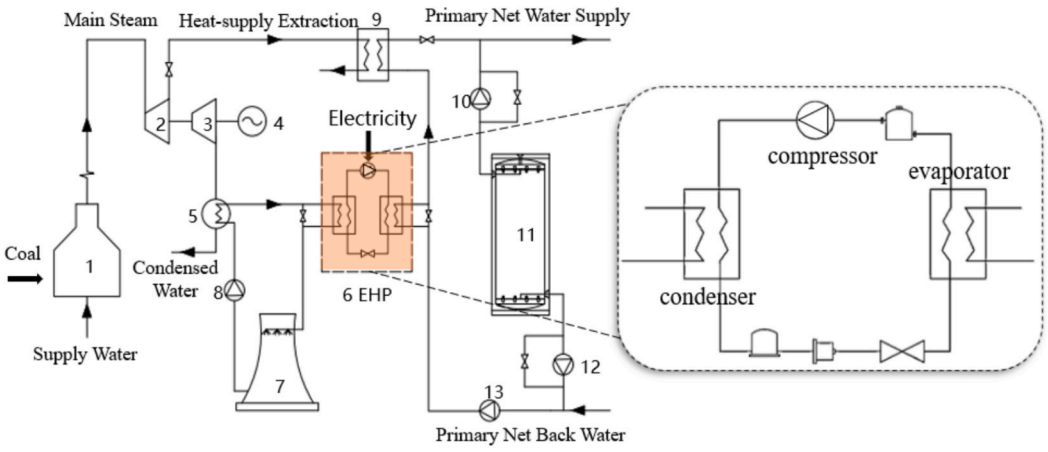

Fig. 2. EHP coupled TES scheme system structure diagram.

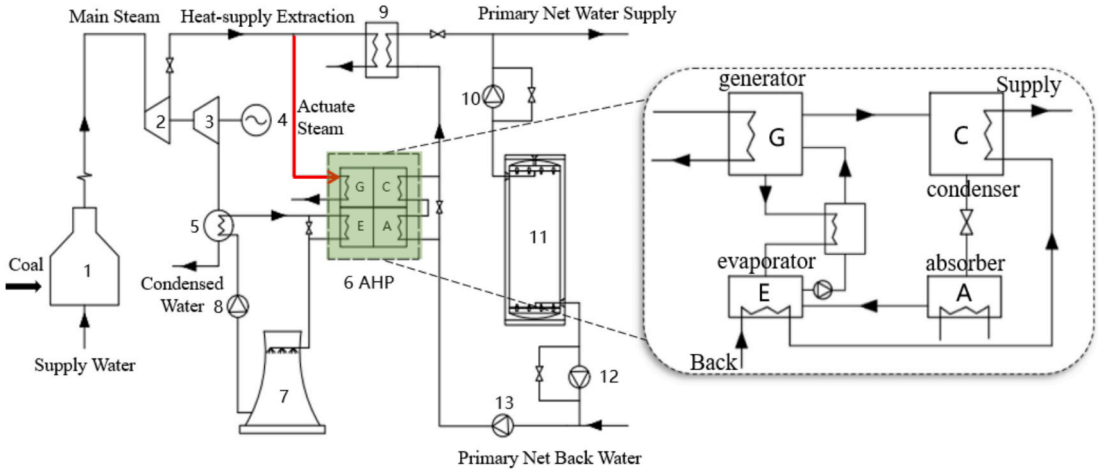

Fig. 3. AHP coupled TES scheme system structure diagram.

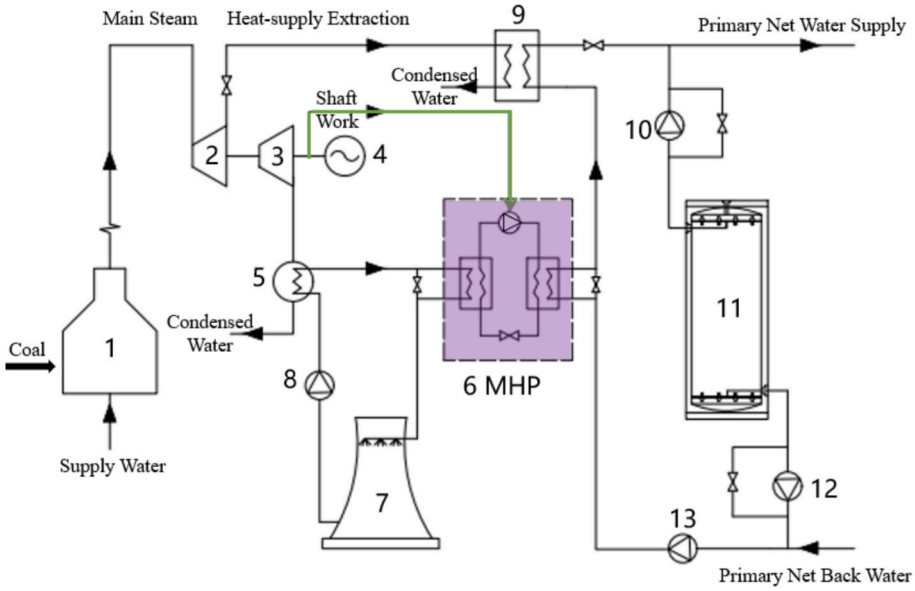

Fig. 4. MHP coupled TES scheme structure diagram.

evaporation side of the AHP is connected to the condensate water circulation system of the thermal power plant and the steam is pumped into the generator for driving, and then heated by the absorber and the condenser for heating. This method raises the upper limit of the units' operation, and improves their thermal conditions.

2.1.4. Mechanical heat pump coupled heat accumulator scheme

MHP is driven directly by mechanical energy[21], reduces energy conversion losses and offers certain advantages over EB and EHP. The mechanical heat pump achieves a COP of 6 under specific conditions, including favorable temperature differentials between the condenser and evaporator. While the thermodynamic principles of mechanical and electrical heat pumps are similar, the mechanical heat pump may exhibit higher performance in scenarios where direct mechanical energy transfer minimizes conversion losses.

In the Fig. 4, MHP directly utilizes mechanical energy for drive, reducing a portion of the power output from CHP units in exchange for more heating. This adjustment helps reduce the thermal output of the units while effectively recovering waste heat from the condensate water of the thermal power plant for heating purposes.

All four schemes incorporate TES to achieve peak shaving and load shifting for both thermal and electric loads. The main difference lies in the operating mechanisms of the driving energy and peak shaving equipment. The EB scheme is unaffected by the thermoelectric ratio, easy to start-up and shutdown. It is suitable for the entire heating period and can directly utilize EB for heating during periods of low heat load before and after heating.

On the other hand, the HP scheme effectively recovers low-temperature waste heat from the thermal power plant, enabling the cascade utilization of energy and enhancing the system's energy utilization efficiency. To maximize the system's operating efficiency and utilize more wind power, the best power and capacity of the peak shaving equipment in the scheme need to be determined through system optimization.

2.2. Optimal scheduling model of integrated thermoelectric peak shaving scheme

In this paper, a traditional mathematical model is developed for the CHP system, with the objective of maximizing the net profit during the heating season. Taking the unique characteristics of different peak shaving equipment into account. On this basis, the optimal scheduling mathematical model of EB, EHP, AHP, MHP, and TES participating in thermoelectric cooperative peak shaving is established.

2.2.1. Modeling of traditional cogeneration system

The traditional CHP system comprises the equipment, including CHP units, pure condensing thermal (CON) units, and a peaking boiler. This section aims to establish the mathematical model and relevant constraints for the heating and power generation of the traditional CHP system.

2.2.1.1. Mathematical model of cogeneration unit. (1) Combined heat and power units planning model.

CHP units are capable of simultaneous electricity and heat production, resulting in significantly improved energy efficiency. The feasible operating region of CHP units is a convex function, where different heat supply corresponds to varying power generation and cost. The characteristic point represents the highest efficiency of CHP units, and they can operate at any two different points within the feasible region as well as any point connected to it [22]. The power output, heating output and operating cost of CHP units are as follows:

$$F_{CHP}(t) = \sum_{i=1}^{I} f_i \bullet x_i(t) F_{CHP}(t) = \sum_{i=1}^{I} f_i \bullet x_i(t) \tag{1}$$

$$P_{CHP}(t) = \sum_{i=1}^{I} p_i \bullet x_i(t) P_{CHP}(t) = \sum_{i=1}^{I} p_i \bullet x_i(t) \tag{2}$$

$$Q_{CHP}(t) = \sum_{i=1}^{I} q_i \bullet x_i(t) Q_{CHP}(t) = \sum_{i=1}^{I} q_i \bullet x_i(t) \tag{3}$$

$$\sum_{i=1}^{I} x_i(t) = 1, 0 \le x_i(t) \le 1 \sum_{i=1}^{I} x_i(t) = 1, 0 \le x_i(t) \le 1 \tag{4}$$

$F_{CHP}(t)$ where $F_{CHP}(t)$ is The operating cost of CHP units at time t, ten thousand yuan; $f_i f_i$ is the operating cost of the i characteristic point of CHP units, ten thousand yuan; $x_i(t) x_i(t)$ is the value of decision variable coding operation in the feasible of CHP units; $P_{CHP}(t) P_{CHP}(t)$ is the electrical output of CHP units at time t, MW; $p_i p_i$ is the electrical output of the i characteristic point of CHP units, MW; $Q_{CHP}(t) Q_{CHP}(t)$ is the thermal output of CHP units at time t, MW; $q_i q_i$ is the thermal output of the i characteristic point of CHP units, MW.

(2) Pure condensing thermal power units planning model.

The operating cost of CON units exhibits a linear relationship with its generating capacity, as demonstrated below [19],

$$F_{CON}(t) = k \bullet P_{CON}(t) F_{CON}(t) = k \bullet P_{CON}(t) \tag{5}$$

$F_{CON}(t)$ where $F_{CON}(t)$ is the operating cost of CON units at time t, ten thousand yuan; kk is the unit power generation cost of CON units, ten thousand yuan/MW ; $P_{CON}(t) P_{CON}(t)$ is t time CON units electrical output, MW.

(3) Planning model of peaking boiler

$$F_{HB}(t) = \frac{3.6 \bullet Q_{HB}(t) \bullet f_{caol}}{\eta_{HB} \bullet q_0} F_{HB}(t) = \frac{3.6 \bullet Q_{HB}(t) \bullet f_{caol}}{\eta_{HB} \bullet q_0} \tag{6}$$

$F_{HB}(t)$ where $F_{HB}(t)$ is the operation cost of the peaking boiler at time t, ten thousand yuan; $Q_{HB}(t) Q_{HB}(t)$ is the thermal output of the peaking boiler at time t, MW; $f_{caol} f_{caol}$ is the standard coal price, yuan /t; $\eta_{HB} \eta_{HB}$ is the operating efficiency of the peaking boiler, %; $q_0 q_0$ is the calorific value of standard coal, 29.27 MJ/kg.

2.2.1.2. Objective function. The objective function of this paper is to maximize the system's operating benefit. The operating income of the thermal power plant primarily comprises revenue generated from the sale of electricity, heat, and wind power. Meanwhile, the operating cost encompasses the operating costs of CHP units, Condensing (CON) units, and the peaking boiler, with the aim of meeting the user's heat demand at the lowest possible operating cost. The objective function can be expressed as:

$$Maxf(x) = F_e + F_h + F_w - F_{cost} Maxf(x) = F_e + F_h + F_w - F_{cost} \tag{7}$$

$$F_h = C_h \times Q_D(t) F_h = C_h \times Q_D(t) \tag{8}$$

$$F_w = C_w \times \sum_{t=1}^{T_{max}} P_w(t) F_w = C_w \times \sum_{t=1}^{T_{max}} P_w(t) \tag{9}$$

$$\begin{aligned} F_e &= C_e \times \sum_{t=1}^{T_{max}} \sum_{i=1}^{I} P_i^{CHP}(t) + C_e \times \sum_{t=1}^{T_{max}} \sum_{j=1}^{J} P_j^{CON}(t) F_e \\ &= C_e \times \sum_{t=1}^{T_{max}} \sum_{i=1}^{I} P_{CHP}^{i}(t) + C_e \times \sum_{t=1}^{T_{max}} \sum_{j=1}^{J} P_{CON}^{j}(t) \end{aligned} \tag{10}$$

$$\begin{aligned} F_{cost} &= \sum_{t=1}^{T_{max}} \sum_{i=1}^{I} F_i^{CHP}(t) + \sum_{t=1}^{T_{max}} \sum_{j=1}^{J} F_j^{CON}(t) + \sum_{t=1}^{T_{max}} F^f(t) F_{cost} \\ &= \sum_{t=1}^{T_{max}} \sum_{i=1}^{I} F_{CHP}^{i}(t) + \sum_{t=1}^{T_{max}} \sum_{j=1}^{J} F_{CON}^{j}(t) + \sum_{t=1}^{T_{max}} F^f(t) \end{aligned} \tag{11}$$

F_e where F_e is the heating season CHP units, CON units sales income, ten thousand yuan/year; F_hF_h is the heating season sales heat income, ten thousand yuan/year; F_wF_w is the income from selling wind power during heating season, ten thousand yuan/year; $F_{cost}F_{cost}$ is the operating cost of the heating system in the season, ten thousand yuan/year; $C_eC_hC_wC_e$, C_h, C_w are the sale of electricity, heat and wind power prices, ten thousand yuan; $P_i^{CHP}(t)P_j^{Con}(t)P_{CHP}^i(t)$, $P_{CON}^j(t)$ are the electrical output of the i CHP units and the j CON units at time t. MW; $Q_D(t)Q_D(t)$ is the system heat load at time t, MW; $P_w(t)P_w(t)$ is the wind power at time t, MW; $F_i^{CHP}(t)F_j^{CON}(t)F^f(t)F_{CHP}^i(t)$, $F_{CON}^j(t)$, $F^f(t)$ are the operating cost of the i CHP units at t time, the operating cost of the j CON units, and the operating cost of the auxiliary heat source equipment, which is ten thousand yuan.

2.2.1.3. System constraint. (1) Constraints on coal-fired cogeneration units.

In addition to the constraints described in Eq. (4), the constraints for coal-fired CHP units also include unit ramping constraints. These constraints limit the increase and decrease of power generation in two adjacent time steps, as well as the upper and lower limits of both heating capacity and power generation, in order to ensure the safe operation of the unit.

$$\left|P_{CHP,i}(t) - P_{CHP,i}(t-1)\right| \le P_{CHP,r}\left|P_{CHP}^i(t) - P_{CHP}^i(t-1)\right| \le P_{CHP,r} \tag{12}$$

$$P_{CHP,min} \le P_{CHP}(t) \le P_{CHP,max}P_{CHP,min} \le P_{CHP}(t) \le P_{CHP,max} \tag{13}$$

$$Q_{CHP,min} \le Q_{CHP}(t) \le Q_{CHP,max}Q_{CHP,min} \le Q_{CHP}(t) \le Q_{CHP,max} \tag{14}$$

$P_{CHP,i}(t)P_{CHP,i}(t-1)$ where $P_{CHP}^i(t)$,$P_{CHP}^i(t-1)$ are t, t-1 time CHP units electrical output, MW; $P_{CHP,r}P_{CHP,r}$ is the climbing power of CHP units, MW/h; $P_{CHP,max}P_{CHP,min}P_{CHP,max}$,$P_{CHP,min}$ are the upper and lower limit of the electric output of CHP units, MW; $Q_{CHP,max}Q_{CHP,min}Q_{CHP,max}$,$Q_{CHP,min}$ are the upper and lower limit of thermal output of CHP units, MW.

(2) Constraint of pure condensing thermal power units.

The constraints for CON units include the upper and lower limits of the unit's electrical output as well as its ramping power limits. These constraints ensure that the electrical output of the CON units remains within specified ranges and that the rate of change in power generation is within acceptable limits:

$$P_{CON,min} \le P_{CON}(t) \le P_{CON,max}P_{CON,min} \le P_{CON}(t) \le P_{CON,max} \tag{15}$$

$$\left|P_{CON,j}(t) - P_{CON,j}(t-1)\right| \le P_{CON,r}\left|P_{CON}^j(t) - P_{CON}^j(t-1)\right| \le P_{CON,r} \tag{16}$$

Where $P_{CON,max}P_{CON,min}P_{CON,max}$, $P_{CON,min}$ are the upper and lower limit of the power output of CON units, MW; $P_{CON,i}(t)P_{CON,i}(t-1)P_{CON}^j(t)$, $P_{CON}^j(t-1)$ are t, t-1 time CON units electrical output, MW.

(3) Peaking boiler confinement.

In order to ensure safety, the operation power of the peaking boiler should be less than the rated power:

$$0 \le Q_{HB}(t) \le Q_{HB,max}0 \le Q_{HB}(t) \le Q_{HB,max} \tag{17}$$

(4) Wind power output constraint.

In the system, the wind power output is less than the wind power forecast:

$$0 \le P_W(t) \le P_{W,pre}(t)0 \le P_W(t) \le P_{W,pre}(t) \tag{18}$$

$P_{W,pre}(t)$ where $P_{W,pre}(t)$ is the forecast amount of wind power at time t, MW.

2.2.1.4. Thermoelectric balance of system. During the operation of CHP system, it is necessary to meet the user's thermal load and electrical load demand, and the thermoelectric balance of the system is expressed by Eqs. (19) and Eqs. (20):

$$Q_D(t) = \sum_{i=1}^{I} Q_i^{CHP}(t) + Q_f(t)Q_D(t) = \sum_{i=1}^{I} Q_{CHP}^i(t) + Q_f(t) \tag{19}$$

$$\begin{aligned} E_D(t) &= \sum_{i=1}^{I} P_i^{CHP}(t) + \sum_{j=1}^{J} P_j^{CON}(t) + P_w(t)E_D(t) \\ &= \sum_{i=1}^{I} P_{CHP}^i(t) + \sum_{j=1}^{J} P_{CON}^j(t) + P_w(t) \end{aligned} \tag{20}$$

$Q_D(t)$ where $Q_D(t)$ is the system heat load at time t, MW; $Q_i^{CHP}(t)Q_{CHP}^i(t)$ is the heat produced by the i CHP unit at time t, MW; $Q_f(t)Q_f(t)$ is the heat supply of auxiliary heat source equipment at time t, MW; $E_D(t)E_D(t)$ is the electrical load on the system at time t, MW.

2.2.2. Mathematical model of heat accumulator

When modeling TES, it is necessary to consider the heat storage equation at time t and the influence of heat storage and heat release rate at time t-1[23]:

$$\begin{aligned} Q_{TES}(t) - Q_{TES}(t-1) &= \eta_{TES,S} \times Q_{TES,S}(t) - Q_{TES,R}(t)Q_{TES}(t) - Q_{TES}(t-1) \\ &= \eta_{TES,S}Q_{TES,S}(t) - Q_{TES,R}(t) \end{aligned} \tag{21}$$

$Q_{TES}(t)Q_{TES}(t-1)$ where $Q_{TES}(t)$, $Q_{TES}(t-1)$ are the heat in TES at t and t-1 time, MW; $\eta_{TES,S}\eta_{TES,S}$ is the heat storage efficiency of the TES, %; $Q_{TES,S}(t)Q_{TES,R}(t)Q_{TES,S}(t)$, $Q_{TES,R}(t)$ are the heat stored and the heat discharged at time t, MW.

Assuming TES runs a cycle, the beginning and the end of the heat storage are the same and are 0:

$$Q_{TES}(0) = Q_{TES}(T_{max}) = 0Q_{TES}(0) = Q_{TES}(T_{max}) = 0 \tag{22}$$

Storage and release power constraints:

$$0 \le Q_{TES,S}(t) \le Q_{S,max}0 \le Q_{TES,S}(t) \le Q_{S,max} \tag{23}$$

$$0 \le Q_{TES,R}(t) \le Q_{R,max}0 \le Q_{TES,R}(t) \le Q_{R,max} \tag{24}$$

$Q_{S,max}Q_{R,max}$ where $Q_{S,max}$, $Q_{R,max}$ are the maximum heat storage and release rate of TES, MW.

2.2.3. Modeling of coupled heat storage system of electric boiler

This section models the system in which the coupled TES of EB participates in the peaking of the unit. The difference between using EB instead of coal-fired boiler for CHP and traditional CHP system is mainly [24]:

(1) Peak load equipment operating costs

$$\sum_{t=1}^{T_{max}} F^f(t) = C_e \bullet \sum_{t=1}^{T_{max}} P_{EB}(t) \sum_{t=1}^{T_{max}} F^f(t) = C_e \bullet \sum_{t=1}^{T_{max}} P_{EB}(t) \tag{25}$$

$P_{EB}(t)$ where $P_{EB}(t)$ is the power consumption of EB at time t, MW.

(2) Electric boiler operation constraints

$$0 \le P_{EB}(t) \le P_{EB,max}0 \le P_{EB}(t) \le P_{EB,max} \tag{26}$$

$$Q_{EB}(t) = \eta_{EB} \times P_{EB}(t)Q_{EB}(t) = \eta_{EB} \times P_{EB}(t) \tag{27}$$

$P_{EB,max}$ where $P_{EB,max}$ is the maximum operating power of EB, MW; $Q_{EB}(t)Q_{EB}(t)$ is the thermal output of EB at time t, MW; $\eta_{EB}\eta_{EB}$ is the operating efficiency of EB, %.

(3) System thermoelectric balance constraints

$$Q_D(t) = \sum_{i=1}^{I} Q_i^{CHP}(t) + Q_{EB}(t) + \eta_{TES,S} \times Q_{TES,S}(t) - Q_{TES,R}(t)Q_D(t) = \sum_{i=1}^{I} Q_{CHP}^{i}(t) + Q_{EB}(t) - Q_{TES,S}(t) + Q_{TES,R}(t) \quad (28)$$

$$E_D(t) + P_{EB}(t) = \sum_{i=1}^{I} P_i^{CHP}(t) + \sum_{j=1}^{J} P_j^{CON}(t) + P_w(t)E_D(t) + P_{EB}(t) = \sum_{i=1}^{I} P_{CHP}^{i}(t) + \sum_{j=1}^{J} P_{CON}^{j}(t) + P_w(t) \quad (29)$$

2.2.4. Modeling of electric heat pump coupled heat storage system

Compared to EB, EHP has a higher operating efficiency and can recover low-temperature waste heat from the condensate water of a thermal power plant for heating purposes. This improves the energy efficiency of the system and enhances its capacity to utilize wind power [15], the difference from the traditional CHP model is:

(1) Auxiliary heat source equipment operating costs.

EHP directly consumes electric energy to drive, so the operating cost is expressed as:

$$\sum_{t=1}^{T_{max}} F^f(t) = C_e \bullet \sum_{t=1}^{T_{max}} P_{EHP}(t) \sum_{t=1}^{T_{max}} F^f(t) = C_e \bullet \sum_{t=1}^{T_{max}} P_{EHP}(t) \quad (30)$$

$P_{EHP}(t)$ where $P_{EHP}(t)$ is t time EHP power consumption, MW.

(2) Electric heat pump operation constraints

$$0 \le P_{EHP}(t) \le P_{EHP,max} 0 \le P_{EHP}(t) \le P_{EHP,max} \quad (31)$$

$$Q_{EHP}(t) = COP_{EHP} \bullet P_{EHP}(t) Q_{EHP}(t) = COP_{EHP} \bullet P_{EHP}(t) \quad (32)$$

$P_{EHP,max}$ where $P_{EHP,max}$ is the maximum power of EHP, MW; $Q_{EHP}(t)Q_{EHP}(t)$ is t time EHP heating output, MW.

(3) System thermoelectric balance constraints

$$Q_D(t) = \sum_{i=1}^{I} Q_i^{CHP}(t) + Q_{EHP}(t) + \eta_{TES,S} \times Q_{TES,S}(t) - Q_{TES,R}(t)Q_D(t) = \sum_{i=1}^{I} Q_{CHP}^{i}(t) + Q_{EHP}(t) - Q_{TES,S}(t) + Q_{TES,R}(t) \quad (33)$$

$$E_D(t) + P_{EHP}(t) = \sum_{i=1}^{I} P_i^{CHP}(t) + \sum_{j=1}^{J} P_j^{CON}(t) + P_w(t)E_D(t) + P_{EHP}(t) = \sum_{i=1}^{I} P_{CHP}^{i}(t) + \sum_{j=1}^{J} P_{CON}^{j}(t) + P_w(t) \quad (34)$$

2.2.5. Modeling of coupled heat storage system of absorption heat pump

AHP is a system that utilizes steam extraction from CHP units to drive. It effectively recovers low-temperature waste heat from the condensate water in thermal power plants for heating purposes. This method helps reduce the heat supply required by the unit. Assuming that all the driving steam is obtained from the heating steam, AHP demonstrates high operating efficiency and can supply a considerable heat. Furthermore, it enhances the flexibility of CHP units.

(1) Auxiliary heat source equipment operating costs.

AHP directly consumes part of the heat supply to be driven by extraction steam, and its operating cost is expressed as:

$$\sum_{t=1}^{T_{max}} F^f(t) = C_h \bullet \sum_{t=1}^{T_{max}} Q_{q,AHP}(t) \sum_{t=1}^{T_{max}} F^f(t) = C_h \bullet \sum_{t=1}^{T_{max}} Q_{q,AHP}(t) \quad (35)$$

$Q_{q,AHP}(t$ where $Q_{q,AHP}(t)$ is t time AHP drive steam heat, MW.

(2) Operating constraints of absorption heat pumps

$$0 \le Q_{q,AHP}(t) \le Q_{q,AHP,max} 0 \le Q_{q,AHP}(t) \le Q_{q,AHP,max} \quad (36)$$

$$Q_{AHP}(t) = COP_{AHP} \times Q_{q,AHP}(t) Q_{AHP}(t) = COP_{AHP} \times Q_{q,AHP}(t) \quad (37)$$

$Q_{q,AHP,max}$ where $Q_{q,AHP,max}$ is AHP's maximum drive steam heat, MW; $Q_{AHP}(t)Q_{AHP}(t)$ is the heating output of AHP at t time, MW.

(3) Restriction of heat supply of combined heat and power units

$$Q_{q,AHP}(t) \le Q_{AHP}(t) \le Q_{AHP,max} Q_{q,AHP}(t) \le Q_{AHP}(t) \le Q_{AHP,max} \quad (38)$$

(4) System thermoelectric balance constraints

$$Q_D(t) + Q_{q,AHP}(t) = \sum_{i=1}^{I} Q_i^{CHP}(t) + Q_{AHP}(t) + \eta_{TES,S} \times Q_{TES,S}(t) - Q_{TES,R}(t)Q_D(t) + Q_{q,AHP}(t) = \sum_{i=1}^{I} Q_{CHP}^{i}(t) + Q_{AHP}(t) - Q_{TES,S}(t) + Q_{TES,R}(t) \quad (39)$$

$$E_D(t) = \sum_{i=1}^{I} P_i^{CHP}(t) + \sum_{j=1}^{J} P_j^{CON}(t) + P_w(t)E_D(t) = \sum_{i=1}^{I} P_{CHP}^{i}(t) + \sum_{j=1}^{J} P_{CON}^{j}(t) + P_w(t) \quad (40)$$

2.2.6. Modeling of mechanical heat pump coupled heat storage system

In this system, MHP utilizes the shaft work of the turbine directly as its driving force. This approach helps minimize mechanical energy losses during the energy transfer process. It reduces the power generation of CHP units while enhancing the flexibility of the unit's peak load operation. Additionally, this setup creates opportunities for integrating wind power into the grid [25].

(1) Auxiliary heat source equipment operating costs.

Since MHP directly consumes mechanical energy to drive, its operating costs are calculated based on the reduced power generation of CHP units.

$$\sum_{t=1}^{T_{max}} F^f(t) = C_e \bullet \sum_{t=1}^{T_{max}} \eta_T \bullet \eta_M \bullet P_{MHP}(t) \sum_{t=1}^{T_{max}} F^f(t) = C_e \bullet \sum_{t=1}^{T_{max}} \eta_T \bullet \eta_M \bullet P_{MHP}(t) \quad (41)$$

$P_{MHP}(t$ where $P_{MHP}(t)$ is t time MHP drive power, MW; $\eta_T\eta_T$ is the transmission efficiency between the turbine and the generator, %; $\eta_M\eta_M$ is the generator efficiency, %.

(2) Mechanical heat pump operation constraints

$$0 \le P_{MHP}(t) \le P_{MHP,max} 0 \le P_{MHP}(t) \le P_{MHP,max} \quad (42)$$

$$Q_{MHP}(t) = COP_{MHP} \times P_{MHP}(t) Q_{MHP}(t) = COP_{MHP} \times P_{MHP}(t) \quad (43)$$

$P_{MHP,max}$ where $P_{MHP,max}$ is the maximum power of MHP, MW; $Q_{MHP}(t)Q_{MHP}(t)$ is the heating output of MHP at time t, MW.

(3) Combined heating and power unit constraints.

Due to the utilization of MHP, the lower limit of CHP power output will be changed:

$$Max(P_{MHP,min}, \eta_T \bullet \eta_M \bullet P_{MHP}(t)) \le P_{MHP}(t) \le P_{MHP,max} Max(P_{MHP,min}, \eta_T \bullet \eta_M \bullet P_{MHP}(t)) \le P_{MHP}(t) \le P_{MHP,max} \quad (44)$$

(4) System thermoelectric balance constraints

$$Q_D(t) = \sum_{i=1}^{I} Q_i^{CHP}(t) + Q_{MHP}(t) + \eta_{TES,S} \times Q_{TES,S}(t) - Q_{TES,R}(t)Q_D(t) = \sum_{i=1}^{I} Q_{CHP}^{i}(t) + Q_{MHP}(t) + \eta_{TES,S} \times Q_{TES,S}(t) - Q_{TES,R}(t) \quad (45)$$

$$E_D(t)+\eta_T \bullet \eta_M \bullet P_{MHP}(t)=\sum_{i=1}^{I} P_i^{CHP}(t)+\sum_{j=1}^{J} P_j^{CON}(t)+P_w(t)E_D(t)$$
$$+\eta_T \bullet \eta_M \bullet P_{MHP}(t)=\sum_{i=1}^{I} P_{CHP}^{i}(t)+\sum_{j=1}^{J} P_{CHP}^{i}(t)$$
$$+P_w(t) \quad (46)$$

The decision variables in this study, which focus on optimizing the operational scheduling of a thermoelectric system, are mainly the heat and power productions of each peak shaving equipment at time step *t*, and thermal energy storage variables, i.e. charging, discharging and storage level at time step *t*. These variables are adjusted within the feasible operational range of each component to achieve the study's optimization objectives: maximizing system efficiency, reducing coal consumption, minimizing carbon emissions, and enhancing wind power integration.

2.3. Case study

To validate the efficacy of the proposed integrated thermoelectric peak shaving model while enhancing the flexibility of CHP units, promoting regional wind power integration, and improving the system's operating income during the heating season, this study employs MATLAB to establish mathematical models for optimal scheduling of various peak shaving schemes. CPLEX optimization software is used to solve the problem.

2.3.1. Example overview

A CHP plant located in Jilin Province is used for validating the developed model. Several key parameters, such as wind curtailment rate, wind power utilization capacity, coal consumption rate, carbon emission reduction rate, exergy efficiency, and energy utilization efficiency, are analyzed and evaluated to assess the performance of the system.

2.3.1.1. Load data. This paper conducts a simulation of a thermal power plant in Jilin Province during the heating season, which spans a total of 183 days (4392 h). The total electrical load demand in the heating season is 3679649MWh, and the total thermal load demand is 2415852MWh. The data regarding wind power forecast, electricity load, and heat load are illustrated in Fig. 5 [26]. It can be observed that the heat load during the heating season exhibits distinct peak and valley periods, with relatively lower heat load before and after the heating period and a substantial increase in heat load during the middle of the heating season. On the other hand, the distribution of electric load uniform throughout the heating season.

2.3.1.2. Equipment parameters of thermal power plant. The plant consists of two 350 MW CHP units, model number C280/N350-16.7/537/537; 2 200 MW CON units, model N200-12.75/535/535; and a 160 MW peaking boiler, operating efficiency of 78 %. The operating characteristic point coordinates and operating costs of CHP and CON units are shown in Table 1 and Table 2. The operating curve of thermoelectric units is shown in Fig. 6.

2.3.1.3. Mathematical model parameters of thermal power plant. The relevant parameter values of the mathematical model of CHP system are shown in Table 3.

2.3.1.4. Model parameters of thermoelectric peaking scheme. The relevant parameters of mathematical models of different integrated thermoelectric peak shaving schemes are shown in Table 4.

3. Results and discussion

In this section, a comparative analysis of the simulation results will be conducted, focusing on the economic aspects, environmental benefits, and wind power utilization.

3.1. Net income from system operation

When calculating the net profit of operating the thermoelectric collaborative peaking system, several factors need to be taken into account. These include the income and operational costs associated with heat sales, electricity sales, and wind power utilization. Additionally, the cost of the new auxiliary heat source equipment needs to be considered. Therefore, in the simulation, it is essential to amortize the cost of the new peak load equipment over its entire lifecycle.

Table 1
CHP units feature point data.

Name	Point A	Point B	Point C	Point D
Electric power /MW	383	267	175	175
Thermal power /MW	0	448	160	0
Running cost /Ten thousand yuan	7.34	7.31	4.39	3.70

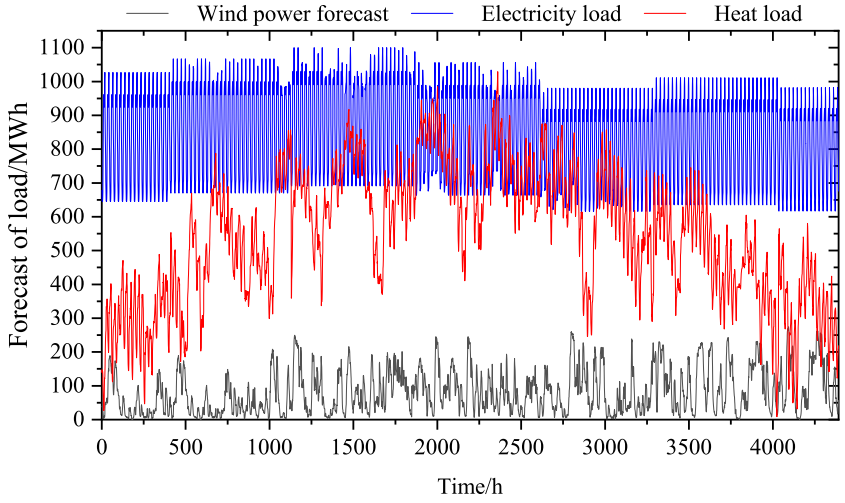

Fig. 5. Heating season load data.

Table 2
CON units feature point data.

Name	Point 1	Point 2
Electric power /MW	100	200
Running cost /ten thousand yuan	2.62	4.71

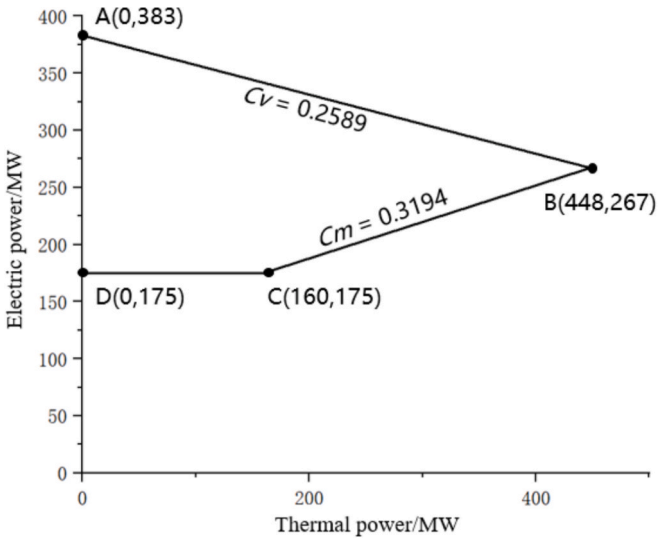

Fig. 6. Operation curve of CHP units.

Table 3
Relevant parameters of mathematical model of CHP system [26].

Parameter	Numerical	Parameter	Numerical
$P_{CHP,r}P_{CHP,r}$	80 MW/h	$P_{CON,r}P_{CON,r}$	70 MW/h
$P_{CHP,max}P_{CHP,max}$	383 MW	$P_{CHP,min}P_{CHP,min}$	175 MW
$Q_{CHP,max}Q_{CHP,max}$	448 MW	$Q_{CHP,min}Q_{CHP,min}$	0
$P_{CON,max}P_{CON,max}$	200 MW	$P_{CON,min}P_{CON,min}$	100 MW
C_hC_h	21.5 yuan/GJ	C_eC_e	373.1 yuan/MWh
C_wC_w	570 yuan/MWh	$f_{caol}f_{caol}$	650 yuan/t
$\eta_{HB}\eta_{HB}$	78 %	$\eta_{TES,S}\eta_{TES,S}$	99.8 %

Table 4
Mathematical model parameters of thermoelectric collaborative peaking scheme.

Parameter	Numerical	Parameter	Numerical
$\eta_{EB}\eta_{EB}$ [27]	99 %	$COP_{EHP}COP_{EHP}$ [28]	6.25
$COP_{AHP}COP_{AHP}$ [29]	1.95	$COP_{MHP}COP_{MHP}$ [21]	6.67
$\eta_M\eta_M$ [25]	95 %	$\eta_T\eta_T$ [25]	95 %

$$F_{tz} = \frac{C_f \bullet R_f + C_{TES} \bullet V_{TES}}{n} F_{tz} = \frac{C_f \bullet R_f + C_{TES} \bullet V_{TES}}{n} \quad (47)$$

F_{tz} where F_{tz} is the cost of amortizing the initial investment of the auxiliary heat source equipment to the entire life cycle of the equipment, ten thousand yuan per year; C_fC_f is the initial investment per unit capacity equipment, ten thousand yuan/MW; R_fR_f is the new peak load equipment capacity, MW; $C_{TES}C_{TES}$ is the cost per cubic meter of TES construction, ten thousand yuan/m^3m^3; $V_{TES}V_{TES}$ is the capacity of TES, m^3m^3; nn is the service life of the equipment is, years, assuming that the service life is 20 years.

The initial investment data of different integrated thermoelectric peak shaving schemes are shown in Table 5.

The above parameters are put into the model of integrated thermoelectric peak shaving scheme for solving, and the net benefits of different schemes are shown in Fig. 7. The net income of the EB coupled TES scheme changes with the power of the EB is shown in Fig(a), where there is a noticeable peak value at 100 MW. The initial investment in the auxiliary heat source equipment affects the net income. In some cases, the net profit after the TES is lower than that without the TES. However, when the TES capacity is 20,000 m3, the system's net income reaches its maximum at 674.85 million yuan. The net income curve of the three HP participating in integrated thermoelectric peak shaving scheme shows a similar trend. As shown in Fig (b), when equipped with 100 MW EHP and 10,000 m3 TES, the highest net income of the system is 725.04 million yuan. The net income of the system with TES is higher than that without TES when the EHP power is relatively small, and the volume change of TES has little impact on the net income of the system operation. However, with the increase of the EHP power, the net income of the scheme without TES becomes significantly higher than that with TES, except for the scheme with a 10,000 m3 TES, and the TES volume has a greater impact on the net income of the system operation. Fig (c) shows that when the driving power of AHP reaches 240 MW, the net income of the system decreases. The net income of the system reaches its peak value of 694.8 million yuan when the TES capacity is 20,000 m3. The larger the capacity of TES, the higher the net income of the system, when the AHP power is relatively small. The initial investment in new equipment reduces the net income of the system compared to that without TES. As shown in Fig (d), the net income curve of MHP is similar to that of EHP. When the MHP power is 110 MW, the net income of the scheme without TES is significantly higher than that with TES. However, when the TES capacity is 10,000 m3, the maximum net income of the system operation is 736.91 million yuan. The influence of the TES capacity on the net operating income of the system increases gradually with the increase of the MHP power.

Table 5
Initial investment data of thermoelectric collaborative peaking scheme.

Parameter	Investment cost
$C_{EB}C_{EB}$ [30]	7.5×10^5 yuan/MW
$C_{EHP}C_{EHP}$ [31]	1.5×10^6 yuan /MW
$C_{AHP}C_{AHP}$ [32]	1.2×10^6 yuan /MW
$C_{MHP}C_{MHP}$ [33]	1.16×10^6 yuan /MW
$C_{TES}C_{TES}$ [26]	0.3×10^6 yuan /m^3

From the perspective of the net operating income of the heating season, MHP and EHP schemes have higher net income, followed by the AHP scheme, and finally, the EB scheme due to the lower operating efficiency of EB and AHP. The MHP scheme achieves higher exergy efficiency due to the efficient conversion of mechanical energy into heat, leading to significant coal savings. The EHP scheme benefits from leveraging low-cost electricity during periods of high wind power availability, thus maximizing wind power utilization and minimizing curtailment penalties. It is evident that the economy of the system will be reduced if the volume of TES or HP power is too large. Therefore, this analysis can optimize the HP and TES capacity for the thermoelectric collaborative peaking system.

3.2. System curtailment rate

When the power generation of the CHP system fails to meet the user's power load demand, a portion of the wind power is utilized as compensation. This helps in reducing the wind curtailment rate of the system and promotes the utilization of regional renewable energy.

$$\eta_W = \frac{P_{W,pre} - P_W}{P_{W,pre}} \times 100\% \eta_W = \frac{P_{W,pre} - P_W}{P_{W,pre}} \times 100\% \quad (48)$$

η_W where η_W is the system curtailment rate, %; $P_{W,pre}P_{W,pre}$ is the forecast amount of regional wind power, MW; P_WP_W is the amount of wind power connected to the system, MW.

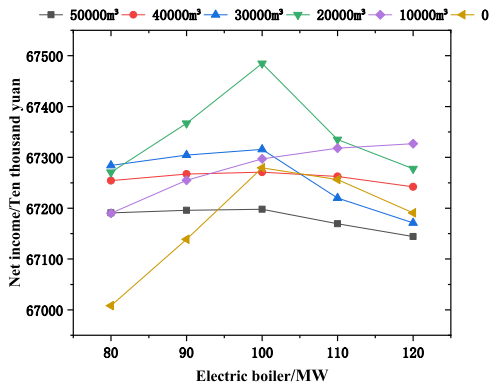

(a) Net benefit of EB coupled heat storage and peak shaving scheme

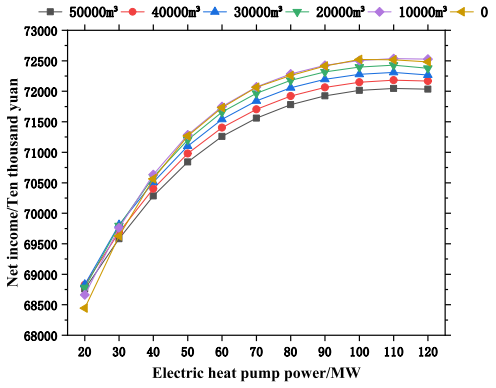

(b) Net benefit of EHP coupled heat storage and peak shaving scheme

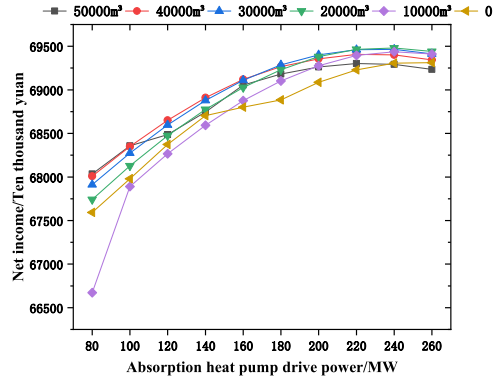

(c) Net benefit of AHP coupled heat storage and peak shaving scheme

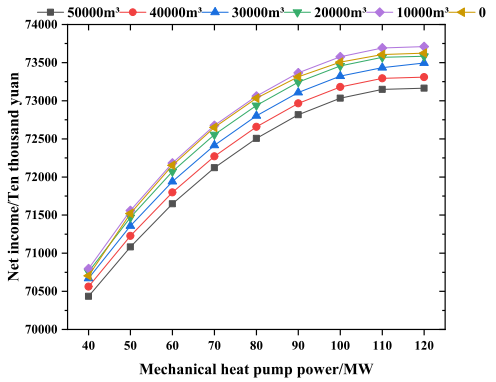

(d) Net benefit of MHP coupled heat storage and peak shaving scheme

Fig. 7. Net benefits of different peak shaving schemes.

The wind curtailment rate of various integrated thermoelectric peak shaving schemes is calculated using the formula mentioned above. To clearly illustrate the difference between the wind curtailment rates of different schemes, the y-axis is standardized, and the calculation results are presented in Fig. 8.

As the capacity of the auxiliary heat source equipment increases, the curtailment rate of the system gradually decreases. There is an inverse correlation between the capacity of the auxiliary heat source equipment and the curtailment rate. In Fig (a) and (b), it can be observed that as the power of the auxiliary heat source equipment increases, the impact of the TES volume on the wind curtailment rate diminishes. A larger TES volume results in a smoother curve for the wind curtailment rate. The EB scheme achieves the lowest wind curtailment rate of 0.1 %, utilizing almost all the wind power. In Fig (c), the AHP scheme exhibits a higher curtailment rate compared to the other schemes. However, the overall trend of the curtailment rate curve remains the same. When the capacity of the auxiliary heat source equipment is small, the change in TES volume has a greater impact on the wind curtailment rate. In Fig (d), the influence of the volume of the heat accumulator on the abandonment rate is small, and the influence is almost negligible compared with that of the auxiliary heat source equipment. From the perspective of the curtailment rate, the EB and EHP schemes directly consume electric energy, while the MHP scheme reduces the electric output of CHP units. Consequently, the curtailment rates of these three schemes are low, thereby weakening the influence of TES on the system curtailment rate.

3.3. *Wind power accommodation*

(1) Wind power utilization

According to the simulation results, the total predicted wind power in the system is 367546MWh. For the traditional CHP system, the wind power on-grid capacity is 276557MWh, as depicted in Fig. 9. The wind power on-grid capacity varies based on different schemes and auxiliary heat source equipment capacities. The upper and lower limits of the rectangle in the Fig represent the maximum and minimum wind power utilization of the system within the range of the auxiliary heat source equipment's capacity. It is evident from the Fig that the AHP scheme has relatively poor wind power utilization. Conversely, the EB scheme exhibits a high level of wind power utilization.

(2) Wind power utilization capacity.

In order to analyze the improvement of system wind power utilization capacity of different schemes after thermoelectric transformation, the concept of system wind power utilization capacity is introduced:

$$\eta_N = \frac{P_W - P_{W,0}}{P_{W,0}} \times 100\% \eta_N = \frac{P_W - P_{W,0}}{P_{W,0}} \times 100\% \tag{49}$$

η_N where η_N is the system's wind capacity, % ; $P_{W,0} P_{W,0}$ is the amount of wind power connected to the traditional CHP system, MW.

The wind power utilization capacity of each scheme after thermoelectric transformation is determined based on the calculations conducted earlier. The results are summarized as follows.

The wind power utilization capacity of the system is directly associated with the capacity of the auxiliary heat source equipment. As

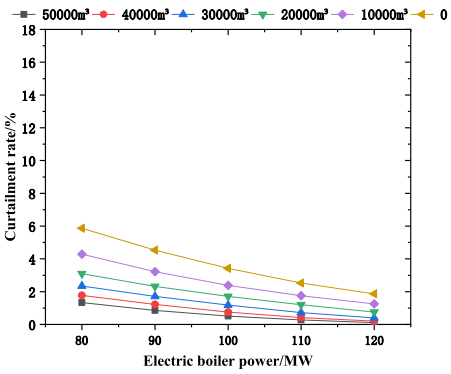

(a) Wind abandonment rate of EB coupled heat storage and peak shaving scheme

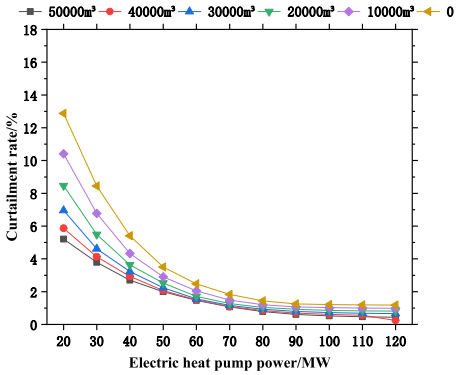

(b) Wind abandonment rate of EHP coupled heat storage and peak shaving scheme

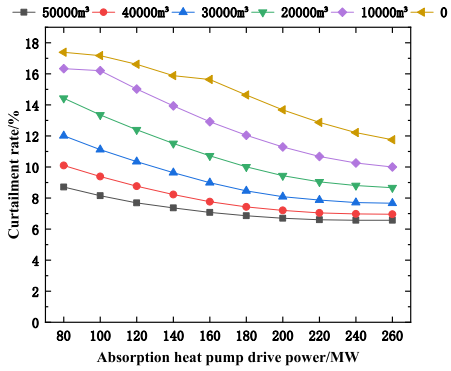

(c) Wind abandonment rate of AHP coupled heat storage and peak shaving scheme

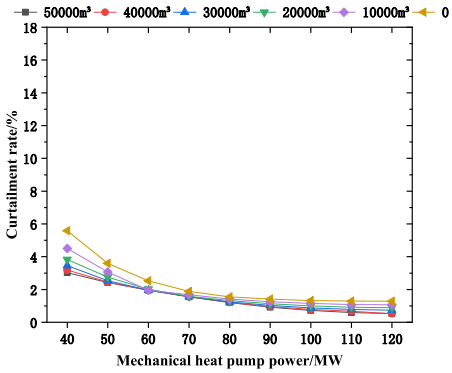

(d) Wind abandonment rate of MHP coupled heat storage and peak shaving scheme

Fig. 8. Wind abandonment rate of different peak loading schemes.

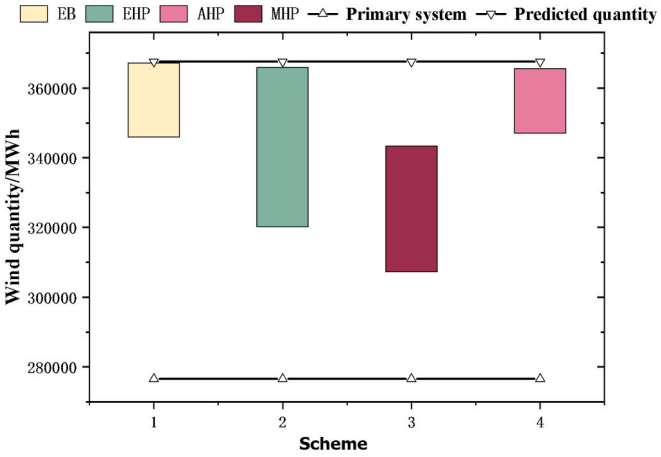

Fig. 9. System wind capacity.

illustrated in the Fig, the wind power utilization curve demonstrates a gradual increase and eventually levels off. In comparison to the original system, both MHP and EHP exhibit higher absorption capacities, with HP improving wind power utilization capacity by at least 24 % and AHP by at least 9.11 %. As the capacity of auxiliary heat source equipment increases, the influence of the TES volume on the system's wind power utilization capacity gradually diminishes. However, for AHP, the volume of TES has a more significant impact on enhancing the system's wind power utilization capacity. In contrast, the volume of TES has little effect on the wind power utilization capacity of MHP. Fig. 10.

3.4. Production unit heat, electricity consumption of coal

In CHP system model, the primary operating cost is associated with coal, and the coal consumption per unit of heat and electricity is a key metric for evaluating cogeneration systems. Based on the simulation results of different schemes and the coal consumption characteristics of CHP and CON units, this section conducts an analysis of various cogeneration collaborative peaking schemes to assess their performance. [34].

$$F_{CON}(t) = a_0 + a_1 \bullet P_{CON}(t) + a_2 \bullet P^2_{CON}(t) F_{CON}(t) = a_0 + a_1 \bullet P_{CON}(t) + a_2 \bullet P^2_{CON}(t) \quad (50)$$

$$F_{CHP}(t) = b_0 + b_1 \bullet P_{CHP}(t) + b_2 \bullet Q_{CHP}(t) + b_3 \bullet P^2_{CHP}(t) + F_{CHP}(t) = b_0 + b_1 \bullet P_{CHP}(t) + b_2 \bullet Q_{CHP}(t) + b_3 \bullet P^2_{CHP}(t) + b_4 \bullet P_{CHP}(t) \bullet Q_{CHP}(t) + b_5 \bullet Q^2_{CHP}(t) b_4 \bullet P_{CHP}(t) \bullet Q_{CHP}(t) + b_5 \bullet Q^2_{CHP}(t) \quad (51)$$

Where $a_0 a_1 a_2 a_0$, a_1, a_2 are the fitting coefficient of coal consumption of CON units; $b_0 b_2 b_3 b_4 b_5 b_0$, b_2, b_3, b_4, b_5 are the fitting coefficient of coal consumption of CHP units..

The fitting coefficients of CHP and CON units are selected in this paper are shown in Table 6 and Table 7.

Eqs. (50) and Eqs. (51) were utilized to calculate the coal consumption of the unit in operation, combined with the system heat

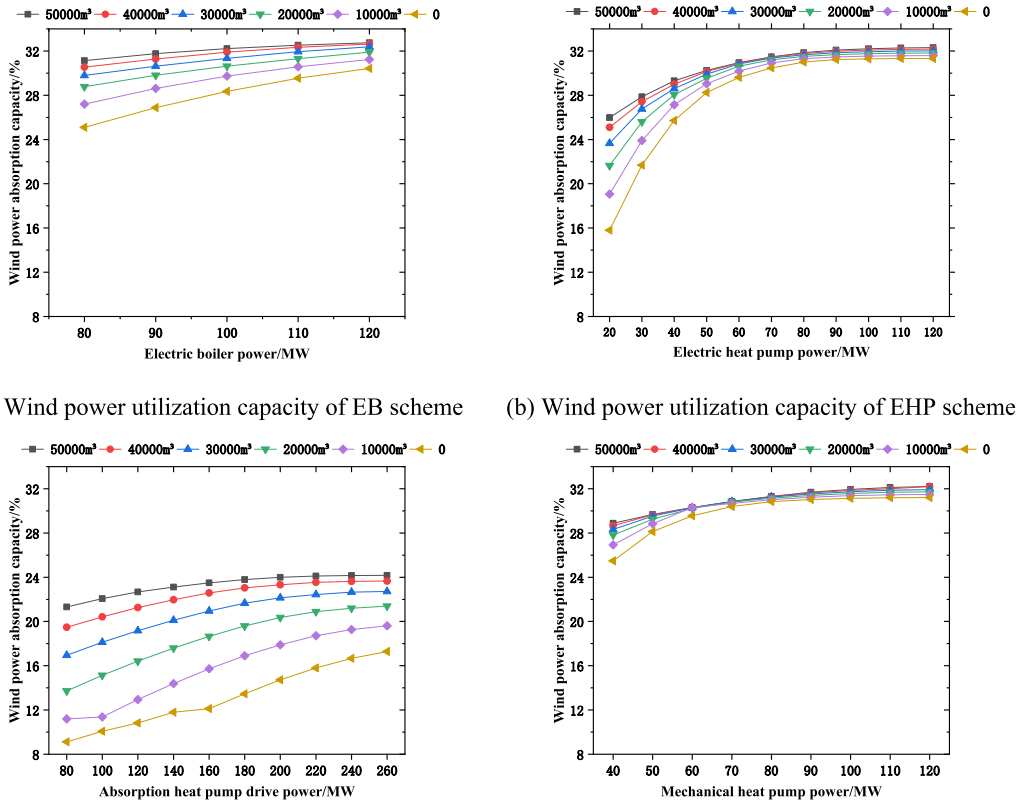

(a) Wind power utilization capacity of EB scheme (b) Wind power utilization capacity of EHP scheme

(c) Wind power utilization capacity of AHP scheme (d) Wind power utilization capacity of MHP scheme

Fig. 10. Wind power utilization capacity of different peak-loading schemes.

Table 6
Fitting coefficient of coal consumption characteristics of CON units.

Name	a_0a_0	a_1a_1	a_2a_2
CON units	11.5370	0.1705	0.00017

Table 7
Fitting coefficient of coal consumption characteristics of CHP units.

Name	b_0b_0	b_1b_1	b_2b_2	b_3b_3	b_4b_4	b_5b_5
CHP units	14.6180	235,592	0.0593	0.000072	0.000037	0.0000048

generation and power generation simulated by the software, and the results were shown in Fig. 11.

Compared to the original system, the EB, EHP, AHP, and MHP solutions can respectively reduce the range of coal consumption per unit of electricity generation is 2.69 kg/MWh, 22.47 kg/MWh, 10.72 kg/MWh, 16.91 kg/MWh. Similarly, the range of coal consumption per unit of heat is, 0.2 kg/GJ, 1.61 kg/GJ, 0.77 kg/GJ, 1.22 kg/GJ. Among these schemes, the capacity of the auxiliary heat source equipment in the EB scheme has minimal influence on reducing the system's coal consumption, while the MHP scheme achieves the maximum reduction in coal consumption.

3.5. Carbon cost reduction rate

Traditional CHP systems have difficulty considering economic, environmental, and energy utilization benefits holistically. To address this issue and respond to the strategic goals of "peak carbon dioxide emissions" and "carbon neutrality," it is crucial to improve the operational efficiency of thermal power plants by promoting collaborative peak shaving of heat and power and regional energy utilization. The cost of the system's carbon emissions should also account for carbon allowances[10].

For CHP units, the thermal output of the unit must be translation to the electrical output of the unit under pure condensing conditions:

$$C_{CHP} = \alpha \bullet (\delta_{CHP} - \gamma) \bullet \sum_{t=1}^{T_{Max}} P_{CHP,d}(t))C_{CHP} = \alpha \bullet (\delta_{CHP} - \gamma) \bullet \sum_{t=1}^{T_{Max}} P_{CHP,d}(t)) \tag{52}$$

$$P_{CHP,d}(t) = P_{CHP}(t) + C_v \bullet Q_{CHP}(t)P_{CHP,d}(t) = P_{CHP}(t) + C_v \bullet Q_{CHP}(t) \tag{53}$$

C_{CHP} where C_{CHP} is the carbon transaction cost of CHP units, ten thousand yuan; $\alpha\alpha$ is the carbon trading price, this paper takes 50 yuan /t CO_2CO_2[35]; $\delta_{CHP}\delta_{CHP}$ is the carbon emission coefficient of CHP units, which is 0.968 kg/kWh in this pipe [36]; $\gamma\gamma$ is carbon trading quota, this article takes 0.798 g/kWh[37]; $P_{CHP,d}(t)P_{CHP,d}(t)$ is the generation power of CHP units at time t under equivalent pure condensation condition, the electric power of CHP units at time t under equivalent pure condensation condition, MW; C_vC_v is the electric power reduced when the unit thermal output of CHP units is increased, MW.

For CON units:

$$C_{CON} = \alpha \bullet (\delta_{CON} - \gamma) \bullet \sum_{t=1}^{T_{Max}} P_{CON}(t))C_{CON} = \alpha \bullet (\delta_{CON} - \gamma) \bullet \sum_{t=1}^{T_{Max}} P_{CON}(t)) \tag{54}$$

C_{CON} where C_{CON} is the carbon trading cost of CON units, ten thousand yuan ; $\delta_{CON}\delta_{CON}$ is the carbon emission coefficient of CON units, which is taken in this paper 0.849 kg/kWh[38].

For wind turbines, wind power is a clean energy, so the carbon

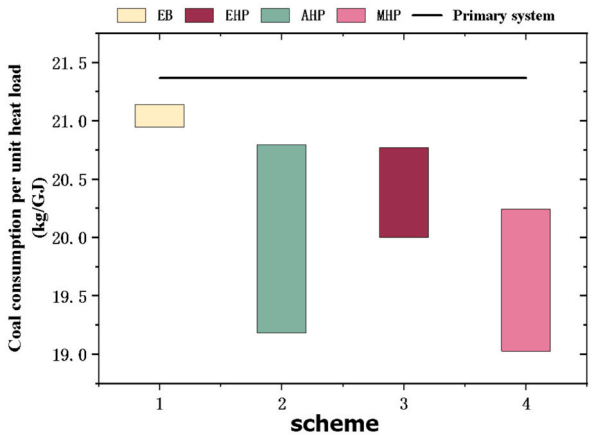

(a) Coal consumption per unit heat of production

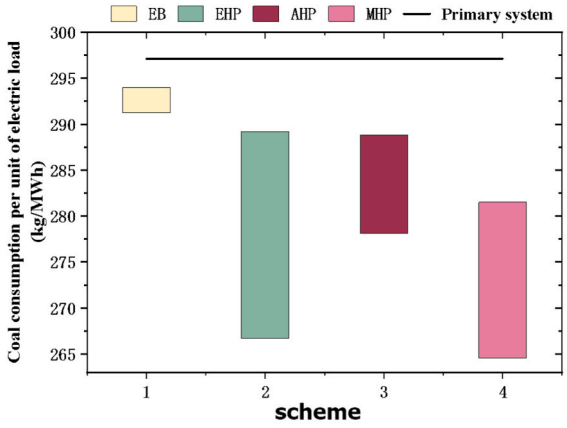

(b) Coal consumption per unit of electricity production

Fig. 11. Production unit heat, electricity consumption of coal.

emissions during its operation are not calculated:

$$C_{Wind} = \alpha \bullet (0-\gamma) \bullet \sum_{t=1}^{T_{Max}} P_{Wind}(t)) C_{Wind} = \alpha \bullet (0-\gamma) \bullet \sum_{t=1}^{T_{Max}} P_{Wind}(t)) \quad (55)$$

C_{Wind} where C_{Wind} is the carbon trading cost of wind power.

Based on the calculations in Eqs. (52), (54), and (55), the original system incurs an operating carbon transaction cost of 17.16 million yuan during the heating season. The addition of auxiliary heat source equipment for thermoelectric transformation is conducive to reducing carbon emissions. The reduction rates of carbon transaction costs for various peaking schemes are illustrated in Fig. 12.

In Fig. 12(a), the EB scheme's reduction rate of over 17.78 % in carbon transaction costs. As the TES capacity increases, the impact of the EB power on the system's carbon transaction cost diminishes. In Fig. 12 (b), when the EHP power is low, the TES volume has a significant effect on the system's carbon transaction cost. The curves for the 40000 m3 and 50000 m3 TES schemes are relatively close, and increasing the TES capacity further does not lead to any changes in the system's carbon trading cost. In Fig. 12(c), the AHP scheme has a lower reduction rate for the system's carbon transaction cost than other schemes, but the TES capacity has a greater influence on the reduction rate. In Fig. 12(d), the MHP scheme curves are relatively smooth, indicating that the impact of the TES volume on the system's carbon transaction cost is negligible. However, the scheme boasts low overall carbon transaction costs and has excellent environmental benefits.

3.6. Exergic efficiency and energy utilization analysis

Exergic efficiency and energy utilization rate are utilized to evaluate cogeneration peaking schemes from both the perspectives of 'quality' and 'quantity'[13].

(1) Exergic efficiency.

It is important to note that different energy sources possess different grades, with heat being classified as low-grade energy and electric energy as high-grade energy. In a cogeneration system, the exergic efficiency of electrical energy plays a crucial role. The exergic efficiency of a CHP system refers to the ratio of the exergic exergy input to the exergic exergy output, which encompasses chemical exergy input as well as electrical and thermal exergy outputs.

Exergic efficiency of CHP system:

$$\eta_{ex} = \frac{E_{out}}{E_{in}} \eta_{ex} = \frac{E_{out}}{E_{in}} \quad (56)$$

η_{ex} where η_{ex} is the exergic efficiency of system, % ; $E_{out}E_{out}$ is the system exited exergy, kW;$E_{in}E_{in}$ is the system entered in the system, kW.

Chemical exergy from standard coal burning:

$$E_{f,CHP} = B_f \bullet q_0 E_{f,CHP} = B_f \bullet q_0 \quad (57)$$

$E_{f,CHP}$ where $E_{f,CHP}$ is the standard coal chemical exergy, kW; B_fB_f is the coal consumption of a CHP system, t; q_0q_0 is the calorific value of standard coal, kJ/kg

System thermal exergy:

$$E_R = E_g - E_h E_R = E_g - E_h \quad (58)$$

$$E_g = D_w[h_g - h_0 - T_0(s_g - s_0)] E_g = D_w[h_g - h_0 - T_0(s_g - s_0)] \quad (59)$$

$$E_{\mathrm{h}} = D_w[h_{\mathrm{h}} - h_0 - T_0(s_{\mathrm{h}} - s_0)] E_{\mathrm{h}} = D_w[h_{\mathrm{h}} - h_0 - T_0(s_{\mathrm{h}} - s_0)] \quad (60)$$

E_R where E_R is the thermal exergy, kW; $E_gE_hE_g$, E_h are the exergy of supply and return water of heat supply network, kW; D_wD_w is the circulating water flow rate of the heat supply network, kg/s; T_0T_0 is the ambient temperature, K; This paper assumes that the room temperature in the heat source plant is 8℃,281.15 K; $h_gh_{\mathrm{h}}h_{\mathrm{g}}$, h_{h} are the enthalpy value of water supply and return of the heat supply network, kJ/kgkJ/kg; $s_gs_{\mathrm{h}}s_{\mathrm{g}}$, s_{h} are the entropy of supply and return water of the heat supply network, kJ/(kg • K)kJ/(kg • K); h_0h_0 is the enthalpy of water at ambient temperature, kJ/kgkJ/kg; s_0s_0 is the entropy of water at ambient temperature, kJ/(kg • K)kJ/(kg • K).

System energy exergy:

$$E_P = P_P E_P = P_P \quad (61)$$

E_P where E_P is the electrical exergy, kW ; P_PP_P is the generating power of units, kW.

Based on the heating data of the thermal power plant, the water supply pressure for the heat supply network is 1.4 MPa, the design water supply temperature and return water temperature are 115℃, 65℃, the circulating water flow of heat supply network is 3146 kg/s. Referring to the enthalpy and entropy chart of water, h_{g}, h_{h}, $h_gh_{\mathrm{h}}h_0h_0$ respectively are 483.62 kJ/kg kJ/kg, 273.42 kJ/kg kJ/kg, 34.21 kJ/kg kJ/kg; $s_gs_{\mathrm{h}}s_0s_{\mathrm{g}}$, s_{h}, s_0 respectively are 3.19 kJ/(kg • K) kJ/(kg • K), 2.65 kJ/(kg • K) kJ/(kg • K), 1.93 kJ/(kg • K) kJ/(kg • K). By inputting these parameters and simulation results into the aforementioned formula for calculation, the exergic efficiency of different schemes is presented in Fig. 13.

As the capacity of auxiliary heat source equipment increased, the exergic efficiency initially rose and then gradually declined. In the EB scheme, when the power of EB is below 110 MW, a larger TES capacity leads to higher exergic efficiency. However, when the power of EB is below 110 MW, a larger TES capacity results in lower exergic efficiency. The capacity of the auxiliary heat source equipment in the EB scheme

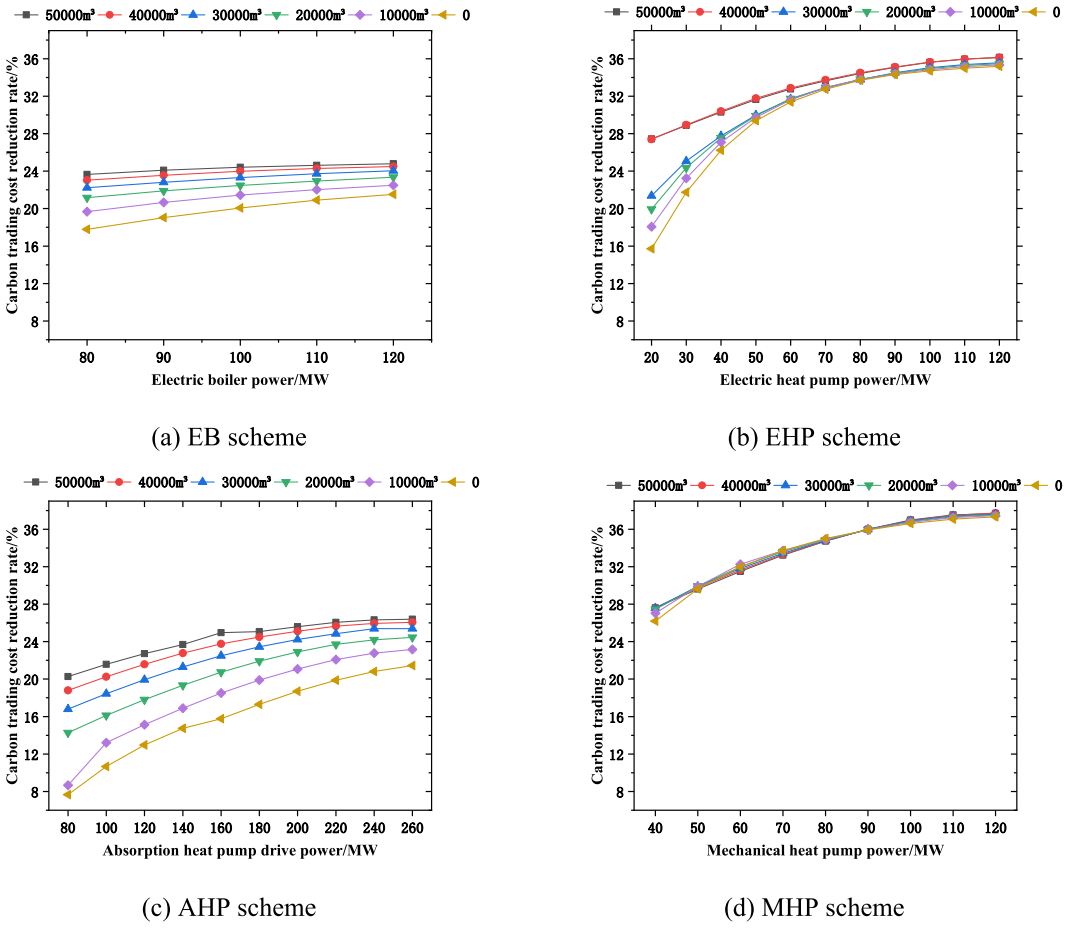

Fig. 12. Carbon trading cost reduction rate of different schemes.

has minimal impact on exergic efficiency, with only a maximum increase of 0.2 %.

In the AHP scheme, the change in TES capacity significantly affects the system's exergic efficiency. For the EHP and MHP schemes, the impact of TES capacity on exergic efficiency is negligible, and a larger capacity of peak regulating equipment leads to higher exergic efficiency, albeit at a slower rate. From the perspective of system exergic efficiency, if the MHP scheme is implemented for integrated thermoelectric peak shaving, there is no need to install TES. For EHP, when the power exceeds 50 MW, increasing TES capacity does not improve the overall system efficiency.

In order to explore the relationship between exergic loss and carbon emission, exergic loss and carbon emission data of four schemes are fitted and analyzed, as shown in Fig. 14.

In the AHP scheme shown in Fig. 14(a), the system's carbon emissions gradually increase with the rise of exergy destruction. As the volume of the heat accumulator increases, the system gains greater peak shaving capacity for heating. At the same time, with the increase in AHP power, the system's carbon emissions gradually decrease, and the rate of increase in carbon emissions slows down. In the MHP scheme, due to the higher COP, the exergy efficiency and carbon emissions are less affected by the volume of the heat accumulator. As seen in Fig. 14(b), the curves of exergy destruction and carbon emissions largely overlap, with only minor differences in slope and intercept. In the EB scheme, shown in Fig. 14(c), increasing the volume of the heat accumulator or the power of EB results in a reduction in both exergy destruction and carbon emissions to varying degrees, with a nearly linear relationship between the two. However, since EB consumes electricity directly for peak heating, its energy efficiency is low compared to that of the heat pump. Consequently, the impact of adding EB on the system's overall exergy efficiency is relatively small. At the same time, as the volume of the heat accumulator increases, the reduction in carbon emissions and exergy destruction occurs at different rates, which leads to the staggered arrangement of the curves in the figure. In the EHP scheme, exergy destruction and carbon emissions are positively correlated as shown in Fig. 14(d). As the volume of the heat accumulator increases, the impact of accumulator volume on the system's carbon emissions becomes negligible when the volume reaches 40,000 m3 or 50,000 m3. As a result, the curves for these two volumes nearly overlap and follow a linear trend. Moreover, with the increase in EHP power, the effect of EHP on both exergy destruction and carbon emissions gradually diminishes. This effect decreases further as the volume of the heat accumulator increases. When the heat accumulator volume is relatively small, the relationship between exergy destruction and carbon emissions appears exponential, with the rate of carbon emissions increasing faster as exergy destruction rises.

(2) Energy efficiency.

The energy utilization efficiency of a system is defined as the ratio of its output energy to input energy. In CHP system, the output energy comprises of the system's power generation and heat supply. The input energy is the heat generated by burning coal. During the CHP transformation process, the system's energy utilization efficiency is improved by adding auxiliary heat source equipment. Fig. 15 illustrates the impact of different auxiliary heat source equipment on the energy efficiency of the system.

The Fig. 15 depicts a rectangle that represents the upper and lower limits of the system's energy efficiency within the simulation range of the auxiliary heat source equipment. The maximum and minimum values of the energy efficiency are shown. From the Fig, it can be observed that the EB scheme has a lower overall energy utilization

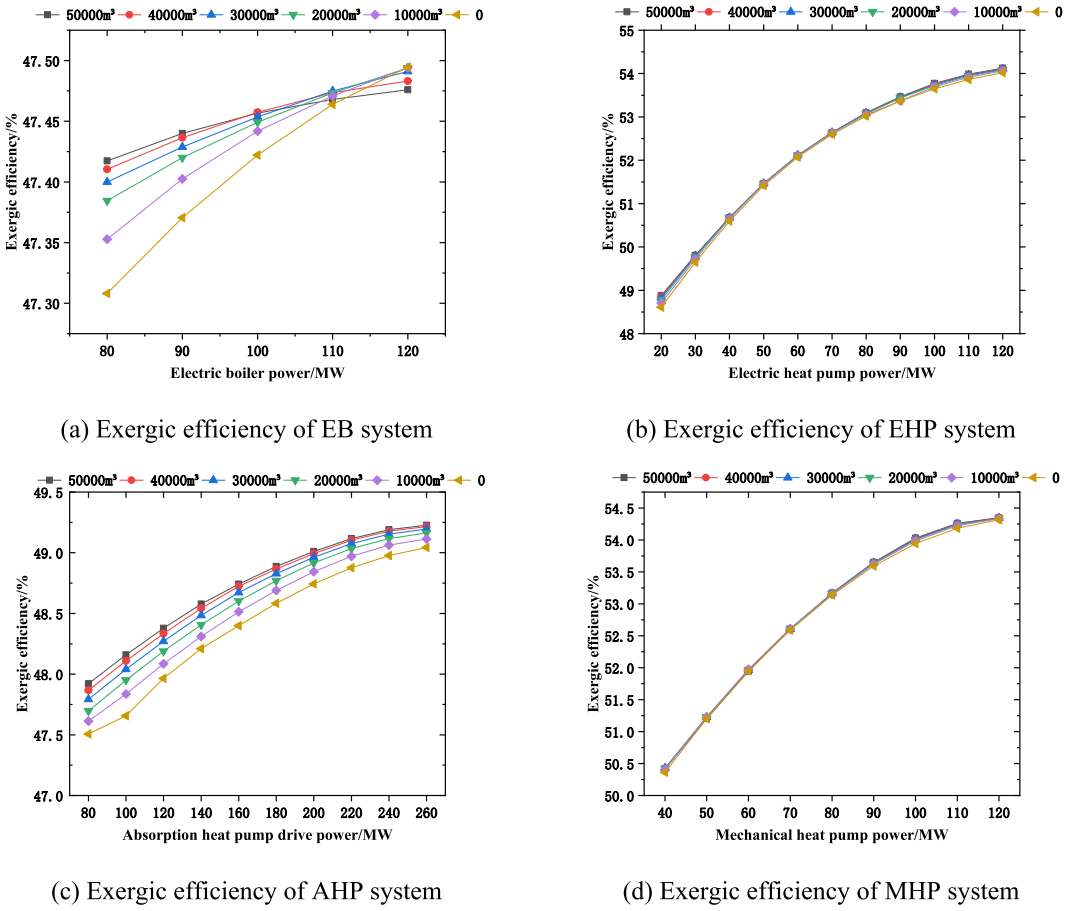

(a) Exergic efficiency of EB system

(b) Exergic efficiency of EHP system

(c) Exergic efficiency of AHP system

(d) Exergic efficiency of MHP system

Fig. 13. Exergic efficiency of different schemes.

efficiency compared to the other schemes, ranging from 63 % to 64 %. On the other hand, both the EHP and MHP schemes exhibit higher overall energy efficiency, surpassing 65 %. The AHP scheme falls in the range of 64 % to 67 % for energy efficiency. The HP scheme is effective in recovering waste heat from the power plant for heating purposes, resulting in a higher system energy efficiency compared to the EB scheme, which solely relies on electric energy for heating. However, the AHP scheme is constrained by operating efficiency limitations, leading to a lower system energy efficiency compared to the EHP and MHP schemes.

4. Conclusions

This study presents an integrated thermoelectric peak shaving framework to enhance renewable energy integration in combined heat and power (CHP) systems. By optimizing the operation of auxiliary heat sources—electric boilers (EB), electric heat pumps (EHP), absorption heat pumps (AHP), and mechanical heat pumps (MHP)—coupled with thermal energy storage (TES), the framework demonstrates significant improvements in system flexibility, efficiency, and environmental performance. The key findings are as follows:

Net Operating Income: The MHP and EHP schemes achieved the highest net benefits, attributed to their superior energy efficiency and reduced operational costs. Optimal configurations include a 110 MW mechanical heat pump with a 10,000 m^3 TES and a 110 MW electric heat pump with the same TES capacity.

Wind Power Integration: The EB scheme exhibited the lowest wind power curtailment rate of 0.1 %, effectively maximizing wind power utilization. Conversely, the AHP scheme, though effective in some scenarios, showed limited capacity for wind power absorption.

Coal Consumption Reduction: Retrofitting CHP systems with auxiliary heat sources reduced coal consumption by up to 16.91 kg/MWh of electricity (MHP) and 1.22 kg/GJ of heat (MHP). The EB scheme showed the least impact on coal savings due to its higher reliance on electricity for heating.

Carbon Emission Mitigation: All schemes significantly lowered carbon transaction costs, with MHP demonstrating the best performance due to its efficient energy utilization. The TES capacity had minimal impact on carbon cost reduction for EHP and MHP, highlighting their inherent efficiency.

Energy Efficiency: The MHP and EHP schemes achieved exergic efficiencies exceeding 65 %, demonstrating superior performance in enhancing system energy utilization compared to EB and AHP schemes.

This research provides insights for improving the operational flexibility of CHP systems and integrating renewable energy sources, offering scalable solutions for regions transitioning to low-carbon energy systems. Future work will focus on extending this framework to

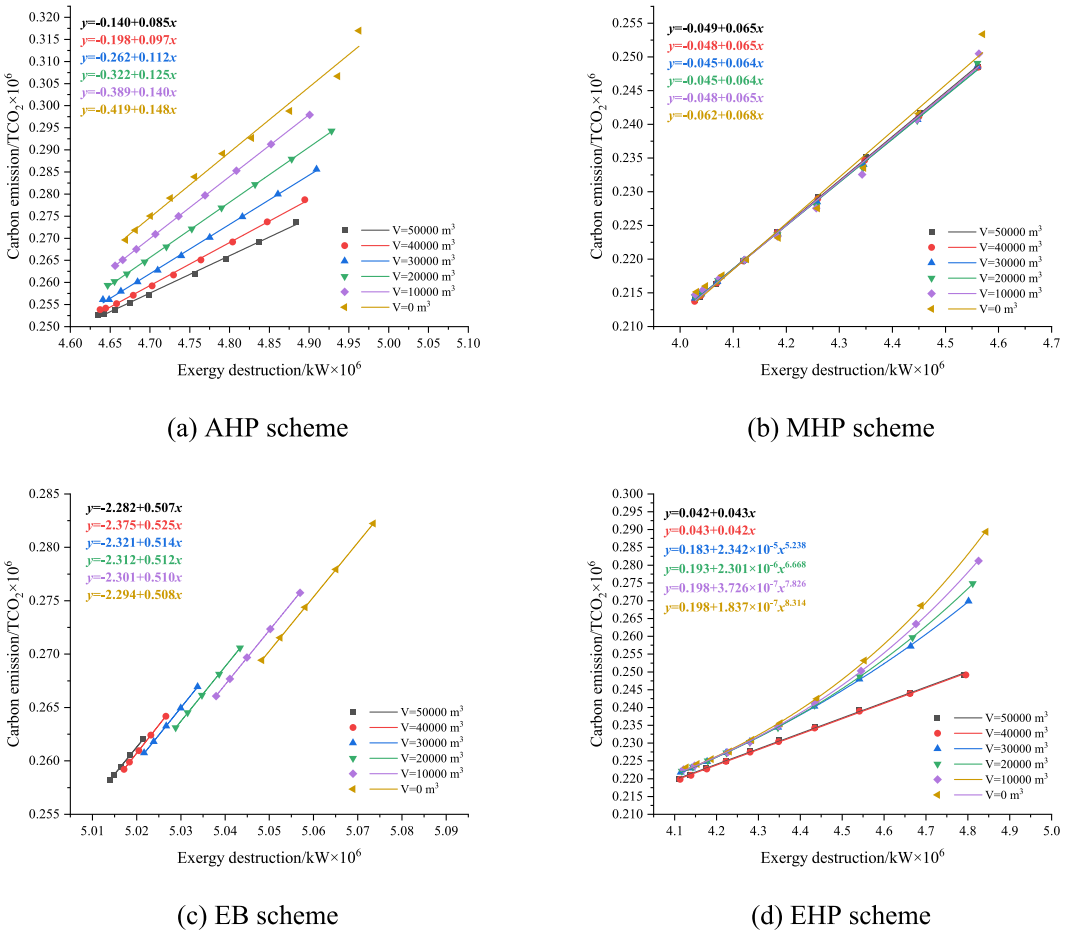

Fig. 14. The relationship between exergy destruction and carbon emission for different schemes.

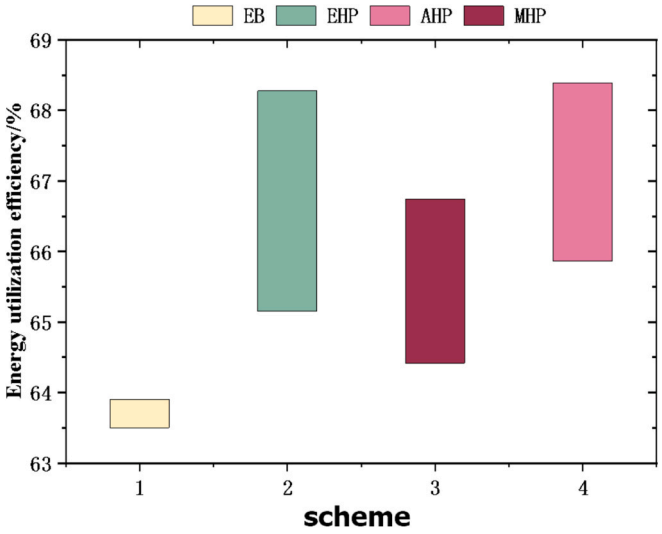

Fig. 15. System energy efficiency of different schemes.

accommodate additional renewable sources, such as solar and biomass, and exploring its applicability in more complex energy systems.

CRediT authorship contribution statement

Haichao Wang: Writing – review & editing, Supervision, Project administration, Funding acquisition, Conceptualization. **Jianbo Han:** Writing – original draft, Visualization, Methodology, Investigation, Data curation. **Tianyu Wang:** Writing – review & editing, Visualization. **Zhiwen Luo:** Writing – review & editing, Investigation. **Risto Lahdelma:** Writing – review & editing, Investigation. **Katja Granlund:** Investigation. **Esa Teppo:** Supervision.

Declaration of competing interest

The authors declare that they have no known competing financial interests or personal relationships that could have appeared to influence the work reported in this paper.

Acknowledgments

This work is supported by the China national key research and development program – China-Finland intergovernmental cooperation in science and technology innovation (Funding No. 2021YFE0116200), academy research fellow funding from Research Council of Finland (Funding No. 336268 and 334205) and NSFC-RS international exchange projects: Digital-twin based smart control of low-carbon heating under climate change (52311530087).

Data availability

Data will be made available on request.

References

[1] China Energy Media Research Institute. China Energy Big Data Report (2022); 2023.

[2] Zhao SF, Ge ZH, Sun J, Ding YL, Yang YP. Comparative study of flexibility enhancement technologies for the coal-fired combined heat and power plant. Energ Convers Manage 2019;184:15–23.
[3] Sun HC, Song MH, Guo PW, Zhang CS, Wang JX. Research on design of heat storage parameters of auxiliary thermal power unit peak load system. Southern Energy Construction 2022;9(3):9–15.
[4] Benalcazar P. Sizing and optimizing the operation of thermal energy storage units in combined heat and power plants: An integrated modeling approach. Energ Convers Manage 2021;242:114255.
[5] Zhang DP, Yue L, Liu FC, Zheng JJ, Xie T, Du PD, et al. Research on the wind power accommodation based on peak shaving by using heat storage electric boiler. In: 2017 IEEE 3rd Information Technology and Mechatronics Engineering Conference; 2017. p. 186–90.
[6] Ling C, Ge Q, Lu J, Ming Z, Song DY. Research on control strategy of electric heat storage boiler based on multi-agent. IEEE International Conference on Power and Renewable Energy 2016;2016:508–12.
[7] Cheng M, Li W, Wang JW, Tian Q, Liu SR, Xiang QL, et al. Control of electric boiler with heat storage for the mitigation of wind curtailment. In: 2020 5th International Conference on Power and Renew Energy; 2020. p. 602–7.
[8] Chen CX, Ge ZH, Zhang YJ. Study of combined heat and power plant integration with thermal energy storage for operational flexibility. Appl Therm Eng 2023;219:119537.
[9] Ayele GT, Tm M, Pierrick H, Björn L, Bruno L. Optimal heat and electric power flows in the presence of intermittent renewable source, heat storage and variable grid electricity tariff. Energ Convers Manage 2012;243:114430.
[10] Xu ZP, Chen J, Zhang JX. Optimization strategy of CSP power plant-electrode boiler-cogeneration combined heating system considering carbon trading. Modern Electronic Technology 2023;46(3):136–42.
[11] Liu M, Wang S, Zhao YL, Tang HY, Yan JJ. Heat–power decoupling technologies for coal-fired CHP plants: Operation flexibility and thermodynamic performance. Energy 2019;188:116074.
[12] Gao S, Li HL, Hou YC, Yan JY. Benefits of integrating power-to-heat assets in CHPs. Appl Energy 2023;335:120763.
[13] Wang ZJ, Gu YJ, Liu HC, Li CY. Comparative analysis of thermoelectric decoupling technology for cogeneration units. Chem Industry Eng Progress 2022;41(7):3564–72.
[14] Wu J. Thermoelectric decoupling scheme and performance analysis of cold, heat and electricity cosupply system [dissertation]. Beijing: North China Electric Power University; 2021.
[15] Wang HC, Hua PM, Wu XZ, Zhang RY, Granlund K, Li J, et al. Heat-power decoupling and energy saving of the CHP unit with heat pump based waste heat recovery system. Energy 2022;250:123846.
[16] Zhang YJ, Ge ZH, Yang YX, Hao JH, Xu L, Du XZ, et al. Carbon reduction and flexibility enhancement of the CHP-based cascade heating system with integrated electric heat pump. Energ Convers Manage 2023;280:116801.
[17] Coşkun S, Motorcu AR, Yamankaradeniz N, Pilat E. Evaluation of control parameters' effects on system performance with taguchi method in waste heat recovery application using mechanical heat pump. Int J Refrig 2012;35(4):795–809.
[18] Nielsen MG, Morales JM, Zugno M, Pedersen TE, Madsen H. Economic valuation of heat pumps and electric boilers in the danish energy system. Appl Energy 2016;167:189–200.
[19] Yang YL, Wu K, Yan X, Cao HY, Long HY. The large-scale wind power integration using the integrated heating load and heating storage control. IEEE Eindhoven Power Tech 2015;2015:1–6.
[20] Zhao XL, Fu L, Wang XY, Sun T, Zhang SG. Modeling and simulation analysis of flue gas waste heat recovery heating system of distributed heat pump peak-regulating gas cogeneration. Acta Energiae Solaris Sinica 2018;39(10):2779–87.
[21] Hu B, Liu H, Jiang JT, Zhang ZP, Li HB, Wang RZ. Ten megawatt scale vapor compression heat pump for low temperature waste heat recovery: Onsite application research. Energy 2022;238:121699.
[22] Wang HC, Yin WS, Abdollahi E, Lahdelma R, Jiao WL. Modelling and optimization of CHP based district heating system with renewable energy production and energy storage. Appl Energy 2015;159:401–21.
[23] Cao LH, Wang ZZ, Pan TY, Dong DF, Hu PF, Liu M, et al. Analysis on wind power accommodation ability and coal accommodation of heat–power decoupling technologies for CHP units. Energy 2021;231:120833.
[24] Yang SH, Sun XP, Tian F, Wu HT. peak shaving of cogeneration boiler. J Shenyang Aerospace ace Univer 2021;38(1):63–9.
[25] Cao CL. Research on direct drive steam compression heat pump system of wind turbine dissertation]. Hebei: North China University of Science and Technology; 2018.
[26] Zhang RY. Research and optimization of integrated technology of thermoelectric peaking in coal-fired thermal power plant to promote the accommodation of wind power [dissertation]. Dalian: Dalian University of Technology; 2020.
[27] Cui Y, Chen Z, Yan YG, Tang YH. Based on the coordinated scheduling model of curtailment and absorption of cogeneration unit with storage heat and electric boiler. Proc CSEE 2016;36(15):4072–80.
[28] Sun J, Liu JY, Tan Z, Ge ZH. Experimental study on low temperature return water achieved by combination of electric heat pump and heat storage. Heating Ventilating & Air Conditioning 2020;50(2):72–5.
[29] Liu JY. Research on planning method of combined heat and power to improve the absorption capacity of wind power [dissertation]. Heilongjiang: Harbin Institute of Technology; 2017.
[30] Rong S. Multi-heat source capacity planning and coordinated scheduling strategy to promote wind power accommodation during heating period [dissertation]. Heilongjiang: Harbin Institute of Technology; 2016.
[31] Fu L, Jiang Y, Zhang YP. Analysis on the application of heating and heating system. J Eng Thermal Energy and Power 2000;15(5):459–63.
[32] Li BL, Hu PF, Zhu N, Lei F, Xing L. Performance Analysis and optimization of a CCHP-GSHP coupling system based on quantum genetic algorithm. Sustain Cities Soc 2019;46:101408.
[33] Tan ZM, Feng X, Yang MB, Wang YF. Energy and economic performance comparison of heat pump and power cycle in low grade waste heat recovery. Energy 2022;260:125149.
[34] Xie BH. Study on coordinated load absorption and abandonment method of electric heating system with pipe network heat storage dissertation. Heilongjiang: Harbin Institute of Technology; 2019.
[35] Zhang XY, Wang LY, Huang L, Wang SH, Wang CT, Guo CX. Considering the expansion of carbon emission flow and carbon bargaining model, the park integrated energy optimization scheduling. Automation of Electric Power Systems 2023;47(9):34–46.
[36] Kang SH, Lu L, Li HQ, Zhang GQ. A novel CHP-HP coupling system and its optimization analysis by genetic algorithm. Energy Procedia 2017;150:2089–94.
[37] Wang ZH, Xu JJ, Tian CG, Cheng L. Combined heat and power dispatching with wind power system including carbon trading cost. Acta Energiae Solaris Sinica 2020;41(12):245–53.
[38] Wang YW, Huang JT, Li XY, Zhuang SX, Xiao B. Multi-objective optimization of cogeneration system based on genetic algorithm. J Shenyang Ins Eng (Natural Science) 2012;8(1):26–9.